https://doi.org/10.5194/cp-2022-23
Preprint. Discussion started: 22 March 2022

Climate of the Past Discussions
Open Access
EGU

Climate and society impacts in Scandinavia following the 536/540 CE volcanic double event

Evelien van Dijk[1], Ingar Mørkestøl Gundersen[2], Anna de Bode[3], Helge Høeg[2], Kjetil Loftsgarden[2], Frode Iversen[2], Claudia Timmreck[4], Johann Jungclaus[4] and Kirstin Krüger[1]

1. Department of Geosciences, University of Oslo, Oslo, Norway
2. Museum of cultural history, University of Oslo, Oslo, Norway
3. Department of Geography, University of Bergen, Bergen, Norway
4. Max Planck Institute for Meteorology, Hamburg, Germany

Correspondence: Evelien van Dijk (e.van.dijk@geo.uio.no), Ingar Mørkestøl Gundersen (i.m.gundersen@khm.uio.no), and Kirstin Krüger (kirstin.kruger@geo.uio.no)

Abstract

In the Northern Hemisphere, the mid-6th century was one of the coldest periods of the last 2000 years, as indicated by both proxy records and Earth System Model (ESM) simulations. This cold period was initiated by volcanic eruptions in 536 CE and 540 CE. Evidence from historical sources, archaeological findings and proxy records suggests that the extent and severity of this volcanic induced cooling was spatially heterogeneous, and that the effect on society resulted in adaptation and resilience at some locations, whereas social crisis has been indicated at others. Here, we study the effect of the volcanic double event in 536 CE and 540 CE on the climate and society in Scandinavia with a special focus on Southern Norway. Using an ensemble of Max Planck Institute ESM transient simulations for 521-680 CE, the temperature, precipitation and atmospheric circulation patterns are studied. The simulated cooling magnitude is then used as input for the growing degree day (GDD) model set-up for Southern Norway. This GDD model indicates the possible effects on agriculture for three different study areas in Southern Norway, representative of typical meteorological and landscape conditions. Pollen from bogs and archaeological records inside the study area are then analysed at high resolution (1-3 cm sample intervals) to give insights into the validity of the GDD model set-up with regard to the volcanic climate impact on the regional scale, and to link the different types of data sets.

After the 536/540 CE double event, a maximum surface air cooling of up to 3.5 °C during the mean growing season is simulated regionally in Southern Norway. With a worst-case scenario cooling of 3 °C, the GDD model indicates crop failures were likely in our northernmost and western study areas, while crops were more likely to mature in the southeastern study area. These results are in agreement with the pollen records from the respective areas. During the sixth century, excavations show an abandonment of farms, severe social impact but also a continuation of occupation or a mix of those. In addition, archaeological findings from one of the excavation sites suggest wetter conditions for the mid sixth century in Scandinavia, as simulated by individual ensemble members. Finally, we discuss the likely climate and societal impacts of the 536/540 CE volcanic double event by synthesising the new and available data sets for the whole Scandinavia.

https://doi.org/10.5194/cp-2022-23
Preprint. Discussion started: 22 March 2022

Climate of the Past Discussions
Open Access
EGU

1. Introduction

Large volcanic eruptions are the largest driver of natural climate variability in the pre-industrial era of the last millenium (Hegerl et al., 2006). Double eruptions or clusters of eruptions that occurred in the last 2000 years coincide with cold periods in the Northern Hemisphere (NH, Briffa et al., 1998; Zhong et al., 2011; Miller et al., 2012; Sigl et al., 2013). One of the coldest decades in Europe and the NH of the last 2000 years occurred during the mid-6th century, which was initiated by the volcanic double event in 536/540 CE. This cold period was discovered in tree-ring and ice core records (Larsen et al., 2008; Büntgen et al., 2011; Sigl et al., 2015), and coincided with historical documents reporting a dimming of the sun in 536 CE (Stothers, 1984; Rampino et al., 1988). Updated ice core chronologies reveal two sulfur peaks that correspond to eruptions in 536 CE and 540 CE (Baillie et al., 2008; Sigl et al., 2015). In addition, a third volcanic eruption occurred in 547 CE (Sigl et al., 2015). This event was relatively small compared to the 536 CE and 540 CE eruptions, but it might have aided in the persistence of the cooling after the volcanic double event (van Dijk et al., 2021 in revision). Tree-ring records from the Alps and Altai recorded a cooling that lasted up to a century and this period has therefore been named the Late Antiquity Little Ice Age (LALIA, Büntgen et al., 2016). However, the extent and duration of the cold period is debated (Helama et al., 2017). More recent climate model studies indicate a multidecadal cooling rather than a centennial one for the NH, likely impacting society in Scandinavia (Toohey et al., 2016; van Dijk et al., 2021 in review). However, the extent of crisis or adaptation by societies in Norway during this time is unknown.

The centuries around the first millennium are characterised by great societal changes, including the ending of antiquity and the beginning of early mediaeval state formations, a process historians believe to have been reinforced by the multidecadal cooling and the outbreak of the Justinian plague in 541 CE (Little, 2006; Rosen, 2006; McCormick et al., 2012). However, less is known about causal relationships between global cooling, regional climate, and local societal changes in Scandinavia.

The 536 CE eruption has been linked to the ‘Fimbulwinter myth’ (Axboe, 1999; 2005; Gräslund, 2008; Gräslund and Price, 2012), in which no summer occurred for three years in a row. Gräslund and Price (2012) interpret the Fimbulwinter myth as a poetic rendition of a profound social crisis during the cooling event. A prolonged summer cooling could have potentially led to widespread crop failure. This is especially true for areas that are already at the temperature limit for growing certain crops, where the effect could be substantial. Evidence for reforestation in different parts of central and northern Europe has been associated with significant changes in the archaeological record and what has been termed the 'Migration Period Crisis' (Welinder, 1975; Berglund et al., 1996; Berglund, 2003; Gundersen, 2019). Based on excavations and dating of several sites in central Sweden, Gräslund and Price (2012) even go as far as to assume that the population in Scandinavia in the mid 6th century may have declined by half.

Other evidence however, suggests that there are regional differences in the climatic impact to this cooling (Degroot, 2021). Several studies highlight the importance of subsistence strategies when discussing societal variability to the cooling event. Communities heavily dependent on cultivation are more likely to have experienced an outright crisis, while those predominantly based on wildlife and pastoralism may have been able to adapt (TeBrake, 1978; Verhulst, 2002; Gräslund and Price, 2012; Tvauri 2014; Hines and Ijssenagger, 2017; Oinonen et al., 2020). These factors are likely to have contributed to considerable regional diversity in disaster impact (Gundersen, 2021).

In Norway, the transition from the Migration Period (400-550 CE) to the Merovingian Period (550-800 CE) occurred right after the volcanic double event in 536/540 CE (Iversen, 2016; Gundersen, 2019). Bajard et al. (2022) reconstructed the agricultural practices from lake sediments in southeastern Norway (lake Ljøgottjern)

https://doi.org/10.5194/cp-2022-23
Preprint. Discussion started: 22 March 2022

and identified a correlation between temperature change and agricultural practices in this area during the Late Antiquity. This result is supported by the study of ter Schure et al. (2021), where analysis of DNA for the same lake sediment led to the same conclusion. However, the landscape in Norway is very diverse, with coastal areas, mountains, and valleys, leading to differences in regional climate and agriculture practices.

In this study, we follow up on van Dijk et al. (2021 in review), and use the Paleo Model Intercomparison Project phase 4 (PMIP4) past2k and the 6th-7th century Max Planck Institute Earth System Model (MPI-ESM) simulations to analyse the atmospheric circulation and surface climate changes as a response to the 536/540 CE eruptions, with a focus on Scandinavia and Southern Norway. Three sites, Fron, Sarpsborg and Høgsfjorden, are selected for case studies with a growing-degree-day (GDD) model, representing different weather and climate regimes and landscapes in Southern Norway. The GDD model utilises the maximum cooling simulated by the MPI-ESM ensemble, and the results are then compared to archaeological- and pollen records to shed more light on the climate, vegetation and societal impacts for Southern Norway. We discuss the likely volcanic climate and society response over Scandinavia based on the climate model data spread, atmospheric circulation patterns, the local archaeology and pollen records next to other available records.

2. Methods

2.1 Climate model simulations

The climate model simulations were run with the MPI-ESM1.2-LR, which is the low-resolution (LR) version used for the Coupled Model Intercomparison Project phase 6 (CMIP6) and the PMIP4. This model version has an atmospheric horizontal resolution of 1.9°x1.9°, and 47 vertical layers, with the top at 0.01 hPa (80 km altitude). The ensemble consists of ten 520-680 CE runs (members 1-10), which were branched off from the past2k (#1) in the year 521 CE by perturbing the atmospheric diffusivity, and two 'past2k' runs (two members, hereafter #11 and #12), following the protocol of Jungclaus et al. (2017). The past2k simulations and the 520-680 CE ensemble are described in more detail by van Dijk et al. (2021 in review). A more complete description of MPI-ESM1.2-LR in its CMIP6 configurations, including parameter and tuning choices, is described in Mauritsen et al. (2019).

2 m air temperature, precipitation, and sea level pressure (SLP) anomalies were calculated by subtracting the multiyear monthly mean of 0 to 1850 CE from the past2k run (#1). From these anomalies, the seasonal means for April to September (the average growing season in Scandinavia) and the ensemble mean were calculated. For the model runs, only monthly values were archived and are available to this study, and therefore we show the growing season mean for the model simulations. 'Two years after the eruption' therefore means the two growing seasons after the eruption. 536-560 CE is taken for the long-term mean, as this is the recovery time after the volcanic double event for temperature. The first two growing seasons after each of the 536 CE and 540 CE eruptions are taken for the short-term response, which is the peak-response time. The significance of the anomalies for the time series was calculated by taking the 2σ (1σ for precipitation) of the control run mean (no volcanic forcing), and the significance for the spatial patterns was calculated by using bootstrapping. For this, random years were taken from the control run to make a time series of 1000 timesteps, which was used to calculate the standard deviation. The 2σ (1σ) was then subtracted from the model ensemble to calculate the significance of the volcanic signal. For more details on this method see van Dijk et al. (2021 in review).

The applied growing degree day model is based on daily mean meteorological observations in Norway from 1961-1990 (Section 2.2). To estimate the relative degree of cooling simulated by the 6th century climate model

https://doi.org/10.5194/cp-2022-23
Preprint. Discussion started: 22 March 2022

Climate of the Past Discussions

runs as input for the GDD model, we used a historical extension of the past2k run (#2) over the historical period. We compare the simulated 1961-1990 mean temperature in the historical run with the meteorological mean temperature anomalies over the study period to get a maximum cooling after the 536 CE and 540 CE eruptions compared to 1961-1990 period (Section 3.1; Table 1).

Table 1. Average temperature in Scandinavia for different ensemble members and periods.

Model run	Time period	Average temperature	Difference to 1961-1990
Historical	1961-1990	8.8 ℃	-
past2k	0-1850 CE	8.4 ℃	-0.4 ℃
521-680 ensemble mean	536-560 CE	7.8 ℃	-1.0 ℃
521-680 ensemble mean	537 CE	7.2 ℃	-1.6 ℃
521-680 ensemble mean	541 CE	6.7 ℃	-2.1 ℃
Individual run max cooling	541 CE	5.3 ℃	-3.5 ℃

2.1.1 Atmospheric circulation analysis

During winter to spring, the climate in Scandinavia is influenced by four winter atmospheric circulation patterns: A positive NAO, a negative NAO, the North Atlantic ridge, and the Scandinavian blocking (Vautard, 1990; Michelangeli et al., 1995; Cassou, 2008). One of the most prominent teleconnection patterns in all seasons is the North Atlantic Oscillation (NAO). It is defined as a high pressure centre over the mid latitudes, generally around Portugal/the Azores, and a low pressure centre over Iceland (Hurrell, 1995). The NAO is associated with changes in the location and intensity of the jet stream, as well as the patterns of heat and moisture transport (Hurrell, 1995). These changes affect the temperature and precipitation patterns over Europe and Scandinavia (van Loon and Rogers 1978).

The atmospheric circulation patterns can be obtained by using empirical orthogonal function calculations and projecting the first 4 modes on the SLP fields (Hurrell 1995). The empirical orthogonal function takes out the most occurring pattern from a data set over time. In this study, the monthly mean SLP from the past2k run #1 is used to calculate the different modes for 0-1850 CE. The SLP anomaly patterns are compared to the four most occurring patterns from this EOF analysis.

2.2 Growing degree day modelling

The accumulated temperature sum during the growing season is usually referred to as 'growing degree days' (GDD). In this study for Scandinavia, 5 °C is used to delimitate the length of the growing season (Fig. 1c, Carter, 1998; Hanssen-Bauer et al., 2017). Local GDD values can then be calculated by using local weather data, which is projected on a terrain model in a geographical information system (ArcGIS) by using a lapse rate of minus 0.6 ℃ for every 100 masl (McIlveen, 1986; Stamnes, 2016; Strand, 1984). Mean daily temperature observations from the Norwegian Meteorological Institute for the standard climate period of 1961-90 are used as baseline values (https://www.met.no/en/free-meteorological-data/Download-services). Grain species have different GDD requirements for reaching maturity, depending on local climate and topographical conditions (Frøseth, 2004; Strand, 1984). In pre-modern times, barley had a basic requirement of approximately 1200-

https://doi.org/10.5194/cp-2022-23
Preprint. Discussion started: 22 March 2022

Climate of the Past Discussions
Open Access
EGU

1350 GDD, oats had 1300-1350 GDD, rye had 1100 GDD, and wheat had 1550 GDD (Foss, 1926). Barley and oat could be sown in either early or late spring, resulting in a wider range of GDD requirements than for rye and wheat. These values must be recalculated for each area in question according to the number of sun hours and precipitation during summertime. Due to more sun hours in northern areas, the required heat budget decreases with approximately 20 GDD per latitude north of 60 ºN (Frøseth, 2004; Strand, 1984; Åssveen & Abrahamsen, 1999). Rainfalls exceeding 250 mm from May to August increase the required temperatures with 60-80 GDD per 100 mm rainfall for barley, 90-100 mm for oats, and 100-110 mm for wheat (Frøseth, 2004).

The three research areas are *Fron,* located in the Gudbrandsdalen valley (eastern inland Norway), *Sarpsborg,* located on the eastern side of the Oslo fjord (southeastern Norway), and *Høgsfjorden*, located in Rogaland (southwestern Norway) (Fig. 1a). The three areas represent three different weather and climate regimes in Southern Norway (Figs. 1 b-c). Several archaeological excavations and field studies have been carried out in these areas (Section 2.3) including pollen analysis from sediment cores with high resolution (Section 2.4). This provides a thorough cultural historical context to analyse and compare the different GDD model output.
By taking these factors into consideration, the local requirements for the three study areas can be defined (Table 2; Gundersen, 2021).

Table 2. Information about the three different sites for the growing degree day modelling, based on local growth conditions and 1961-90 meteorological data for each area.

Area	Mean summer precipitation	Latitude	Barley requirements	Rye requirements	Oats requirements	Wheat requirements
Fron	230 mm	61.5 °N	1169-1319 GDD	1069 GDD	1269-1319 GDD	1519 GDD
Sarpsborg	277 mm	59.2 °N	1234-1384 GDD	1115 GDD	1341-1391 GDD	1594 GDD
Høgsfjorden	434 mm	58.8 °N	1351-1501 GDD	1123 GDD	1497-1547 GDD	1766 GDD

In this study, two definitions for growing season are used. For the MPI-ESM simulations, monthly mean data are available to create a *mean* growing season, where the months April to September are taken. The definition of the actual growing season however, is the number of days with a temperature at or above 5 ℃, which can be different from year to year. This is referred to as the *active* growing season (Carter, 1998).

2.3 Archaeological setting, data, and study areas

The three selected study areas were parts of larger 'tribal' areas in the Roman and Migration periods (200–550 CE), which turned into petty kingdoms in the Merovingian and Viking periods (550-1050 CE), and gradually became integrated in the realm of the Norwegian kingdom ca. 900–1020 CE. 1500 years ago, the Scandza peninsula, which included present-day Sweden and Norway, was home to at least 25 tribal communities. According to the learned Greek Procopius (1919 [~530-560], Book XIV and XV), written in the mid-6th century, there were 'thirteen very numerous nations' (nationes) in Thoulē (which equals to Scandza), one of which was probably the people Chaideinoi of Hedmark that the Fron area probably belonged to (Iversen, 2020). The peoples of Vikverir held land in the historic region Viken, where the lost mediaeval country Vingulmark, contains the Sarpsborg area, while the Høgsfjorden area is located among the people of Rugi in Rogaland. Over the next 500 years, these ‘numerous nations’ united into two larger kingdoms: Norway and Sweden (Brink 2008a; Andersson 2009; Iversen 2020).

https://doi.org/10.5194/cp-2022-23
Preprint. Discussion started: 22 March 2022

Climate of the Past Discussions
Open Access
EGU

Fron area

Fron is is the northernmost of our case study areas, and it is located in the narrow Gudbrandsdalen valley (Fig. 1a). In history, the Heiner (heiðnir) tribe is first mentioned in written sources around 150 CE, referred to as Chaideinoi by the Greco-Roman astronomer, geographer and mathematician Claudius Ptolemy (Andersson, 2009). Their territory, Hedmark (Heiðmǫrk), may in addition to modern-day Hedmark have included the valleys of Gudbrandsdalen and Østerdalen, as it did in the Viking Age (800–1050 CE) (Iversen and Brendalsmo 2020; Iversen 2021).

With Christianity arriving through warlike political campaigns in the early 1000s CE, the petty kingdom of Hedmark disappeared and the area was divided in administrative units called þriðjungar. A þriðjung was a large legal district, comparable to a county. Þriðjungar are first recorded in the early 11th century, but are likely to be of ancient origin. The Fron area is located north in the þriðjung Søndre Gudbrandsdalen (Fig. 1a) which borders the þriðjung Nordre Gudbrandsdalen to the north and þriðjung Hedmark and Østerdalen to the south. During the Viking- and middle ages (800–1500 CE) and potentially earlier, these three districts had a common popular thing (legal assembly) at Åker, Vang (first recorded in connection with events 1046/47 CE).

This area has a lower accumulated growing degree count for the growing season compared to the other two areas, and the second lowest summer precipitation of the study areas. The local wind direction is dependent on the valley orientation, which is east-west, leading to a prevailing wind from the west (Fig. A5a).
The bog located in this area is Ulbergmyr and is further described in Section 2.4 (Fig. 1a).

Sarpsborg area

The Sarpsborg research area (Fig. 1a), is located south in the mediaeval county of Vingulmark, which included the coastal land from Sweden to Vestfold. To the east, Vingulmark bordered Ranrike (Båhuslen) and Värmland, to the north to Romerike, Ringerike and Numedal, and to the west to Vestfold (Munch, 1849). The last mention of Vingulmark is made by the Icelandic historian Snorri Sturluson (Hkr, stanza 73) in *Kringla heimsins* in connection with events in king Olav Haraldsson's time, i.e. early 1000s CE. From other sources, we know that Vingulmark still functioned as a county around 1177 CE (Indrebø, 1932; Pedersen et al., 2003). The county was later divided in two separate parts.

This area has quite high accumulated temperature for the growing season, and has the lowest summer precipitation of all three case studies (Figs. 1b-c). The wind direction is mainly from the south or west, but because this area is flat, it is more variable than for the other two case study areas, as the wind direction is not confined by the topography of the landscape (Fig. A5b).

The bog used for the pollen analysis in this area is Haraldstadmyr (Fig. 1a, Section 2.4).

Høgsfjorden area

The Høgsfjorden research area is located east in the county of Rogaland. In *De origine actibusque Getarum*, the so-called *Getica* (551 CE), Jordanes lists about 25 tribes living in Scandinavia (excluding Denmark), including the Rugi (Ryger, Norway) (Aetel Rugi = the main Rugir). The place-name specialist Stefan Brink (2008) accept the identification of the Rugi as ‘the people living in Rogaland’. The name Rogaland derivates from the peoples’ name, meaning the 'rye-growers'. The poem Widsith, composed c. 550 CE, also mentions the Rugus. The poem was written down in the 7th century, but has only survived in a 10th century manuscript (Malone 1962; Neidorf 2013).

This area has a similar length of the growing season as the Sarpsborg area, but higher summer precipitation, which leads to higher growing degree days required for the different crops (Figs. 1b-c, Table 2). The annual mean wind direction is from the west. Because of the fjords, the local wind direction is directed by the shape

https://doi.org/10.5194/cp-2022-23
Preprint. Discussion started: 22 March 2022


Climate of the Past Discussions

and orientation of the valley. For the Forsand valley, where the excavation sites and the bog are, this means the wind comes from the southwest or the northeast. No meteorological station is available for this fjord, so data has been taken from a nearby valley with a similar orientation (Fig. A5c).

The bog in this area is Åsheimmyr (Fig. 1a, Section 2.4)

The length of the active growing season (based on 1961-1990 data) for the three different case study areas are shown in Fig. 1b. From this map, we can see that the growing season is the longest at the coast, and shortest in the inland valleys of Southern Norway.

2.3.1 C14 data

The collected radiocarbon dates come from different contexts, such as buildings, clearance cairns, agricultural layers and a variety of other settlement remains. However, cooking pits are excluded from the study, as they represent a temporally restricted cultural phenomenon in Norwegian archaeology (Gundersen, Rødsrud, & Post-Melbye, 2020). They are mostly associated with the Early Iron Age (500 BCE-550 CE) and frequently used for dating purposes, thus creating an overrepresentation of Early Iron dates in the overall record. Likewise, we have omitted radiocarbon dates from iron production sites, including the charcoal pits integral to iron production. Data from these sites may skew the data as most iron production sites are from the 900–1300 CE and almost exclusively in certain inland regions (Loftsgarden 2020).

To model the C14 dates, we have used the Summed Probability Distributions (SPD) analysis within the rcarbon package (Crema and Bevan 2020) in the R statistical programming language (R Core Team, 2019). Dates were calibrated using the Intcal20 calibration curve (Reimer et al., 2020). All dates are presented as calibrated dates BCE/CE. In order to mitigate bias of well-researched areas and well-dated sites, we have structured the dates into bins with cut-off value at 50 years at the site level prior to the SPD analysis. The method and data are further described by Loftsgarden and Solheim (in press).

https://doi.org/10.5194/cp-2022-23
Preprint. Discussion started: 22 March 2022

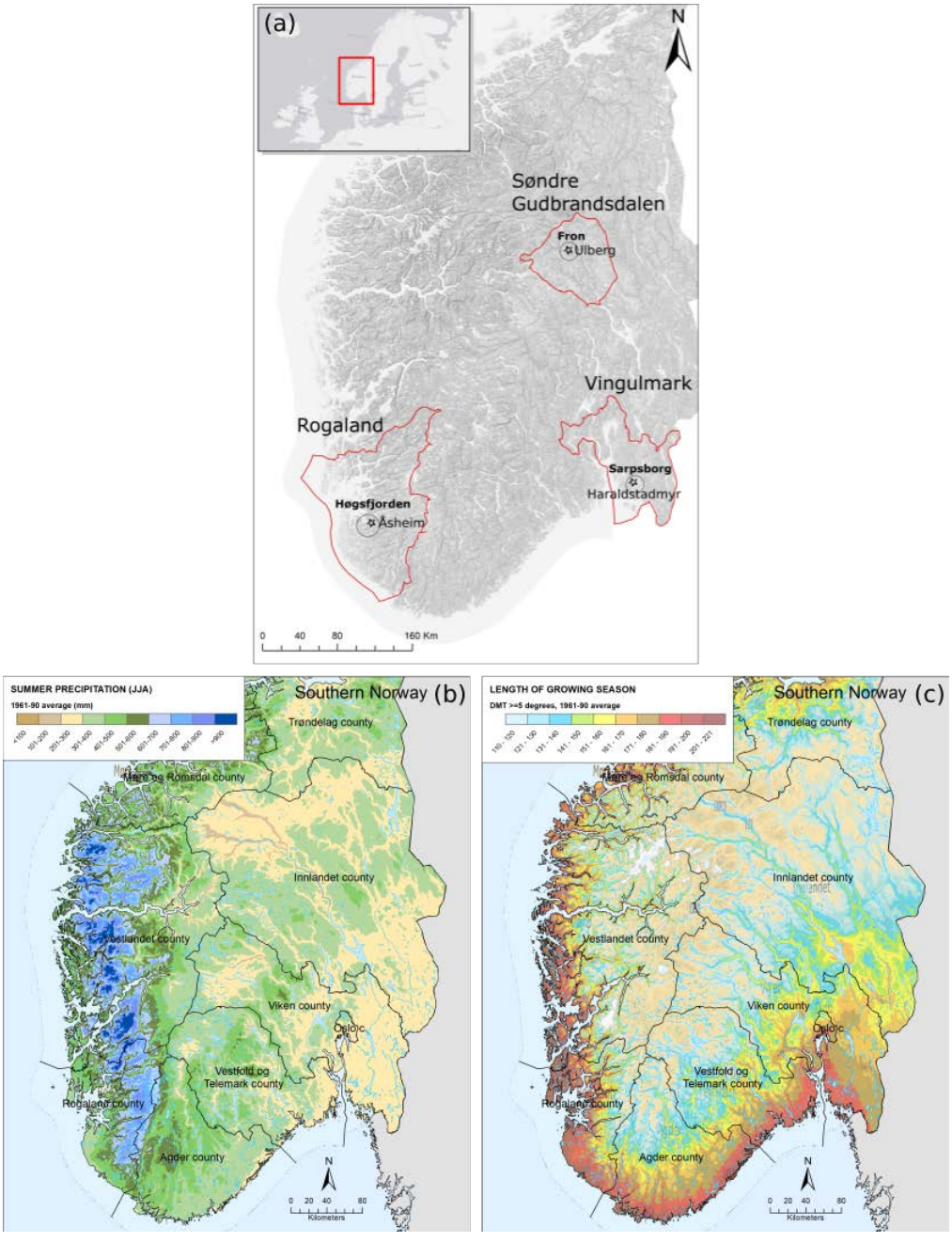

290

Figure 1. a) The three areas and sites for the case study. Red outline indicates the regions, bold names are the areas and the stars indicate the locations and names of the bogs analysed for pollen. DEM map from ESRI 2020. b) The summer precipitation and c) average length of the growing season (days) for Southern Norway during 1961-1990, for days with a daily mean temperature (DMT) at or above 5 °C (adapted from Hanssen-Bauer et al., 2017).

https://doi.org/10.5194/cp-2022-23
Preprint. Discussion started: 22 March 2022

Climate of the Past Discussions
Open Access
EGU

295 **2.4 Pollen analysis**

Pollen analyses were carried out from three different peat bogs in Haraldstadmyr, Ulbergmyr and Åsheimmyr (Table 3). The cores were sampled with a Russian corer from the deepest parts of the bogs (Høeg, 1999; de Bode, 2021; and Gundersen, 2021).

300

Bulk samples for radiocarbon dating were dated by Lund University Radiocarbon Dating Laboratory and Tandem Laboratory at Uppsala University, and calibrated using the IntCal20 calibration curve (Reimer et al., 2020). The age-depth model was generated using R software and the R code package 'Bacon' 2.4.3 (Blaauw and Christen, 2011).

305

Approximately 1 cm^3 of peat was collected for each pollen sample, at intervals varying from 1 cm to 20 cm. For each peat sequence, 1-3 cm intervals (~8-24 years resolution) were used for the depths corresponding to the time period 250-1150 CE in order to obtain a high resolution palynology for this time period. Pollen percentages were calculated based on the pollen sum (ΣP), which expresses the total terrestrial pollen taxa.
310 Percentages of the local and aquatic pollen types, as well as most of the spore plants and the number of charcoals, were calculated based on ΣP+X, where X represents the pollen type, spore or charcoal in question. The pollen diagrams were plotted using R version 4.0.3 (2020-10-10) with packages 'rioja' version 0.9-26 (Juggins 2020), 'ggplot2' version 3.3.3 (Wickham 2016), 'tidyverse' version 1.3.0 (Wickham et al., 2019) and 'neotoma' version 1.7.4 (Goring et al., 2015). The percentages were plotted against their corresponding mean
315 ages as generated by the age-depth model (Section C in the Appendix).

Table 3. Information about the three peat sequences collected for pollen analysis.

Site name	Date of coring	Coordinates location	Altitude (m.a.s.l.)	Depth (cm)	Sample intervals (cm)	Resolution (yrs)	No. samples
Haraldstadmyr (Sarpsborg area)	May 2018	59°17'42.1"N, 11°03'18.3"E	42	0-282	Varying from 1-20. For depths 80-126: 1.	For depths 80-126 cm: c. 14	82
Ulbergmyr (Fron area)	June 2019	61°33' 4.6"N, 9°54' 36.4"E	275	0-495	Varying from 1-10. For depths 25-130: 1-3.	For depths 25-130 cm: c. 8-24	83
Åsheimmyr (Høgsfjorden area)	June 1982	58°54' 4.7"N, 6°7' 17.7"E	115	30-950	Varying from 2-10. For depths 240-416: 2.	For depths 240-416 cm: c. 13	165

320

https://doi.org/10.5194/cp-2022-23
Preprint. Discussion started: 22 March 2022

3. Results

3.1 6th century climate

In this section, the results are given for the simulated 6th century climate response to the volcanic double event of 536/540 CE, where the focus is on the mean response for the growing season (AMJJAS) in Scandinavia. To gain insight into the relationship between the volcanic impact and the climate response, the NH extratropical aerosol optical depth (AOD) is shown for the study period, where four large eruptions in 536 CE, 540 CE, 574 CE, and 626 CE are visible as large peaks, indicating a more opaque sky (Fig. 2a). The climate model simulations reveal a widespread cooling for the growing season after the 536 CE and 540 CE eruptions in the NH extratropics, which results in an ensemble mean cooling of about 2 °C (Fig. 2b). The cooling remains significant for 10 years after the 540 CE eruption and returns to the mean temperature from ~555 CE onwards. Temperatures for Scandinavia show a maximum cooling of ~1.5 °C after the 536 CE and 540 CE eruptions, but also a larger internal variability of 1.2 °C compared to 0.4 °C for the NH extratropical mean, which leads to a less distinct volcanic signal. Only the first year after the eruption ensemble mean is the 2m air temperature is outside the range of internal variability, whereas it takes up to 20 years (until 560 CE) for the temperature to return to the mean value (Fig. 2c).

For the NH extratropics, precipitation decreases after the volcanic double event by 3 mm month^{-1} (Fig. 2d), which is a significant reduction (on the 1σ level). For Scandinavia, this is up to 7 mm month^{-1}. However, just as with temperature, the volcanic signal on precipitation is only significant right after the eruptions due to high internal variability over Scandinavia (Fig. 2e). After the 540 CE eruption, it takes approximately ten years for the precipitation anomaly to return to 0.

During the maximum volcanic induced cooling over Scandinavia, the ensemble mean growing season temperature decreases to the absolute value of 6.9 °C. However, this is the ensemble mean as well as a spatial mean. To gain insight in the regional response we analyse the spatial temperature and precipitation distribution after the volcanic double event for both the long term and the short term response.

https://doi.org/10.5194/cp-2022-23
Preprint. Discussion started: 22 March 2022

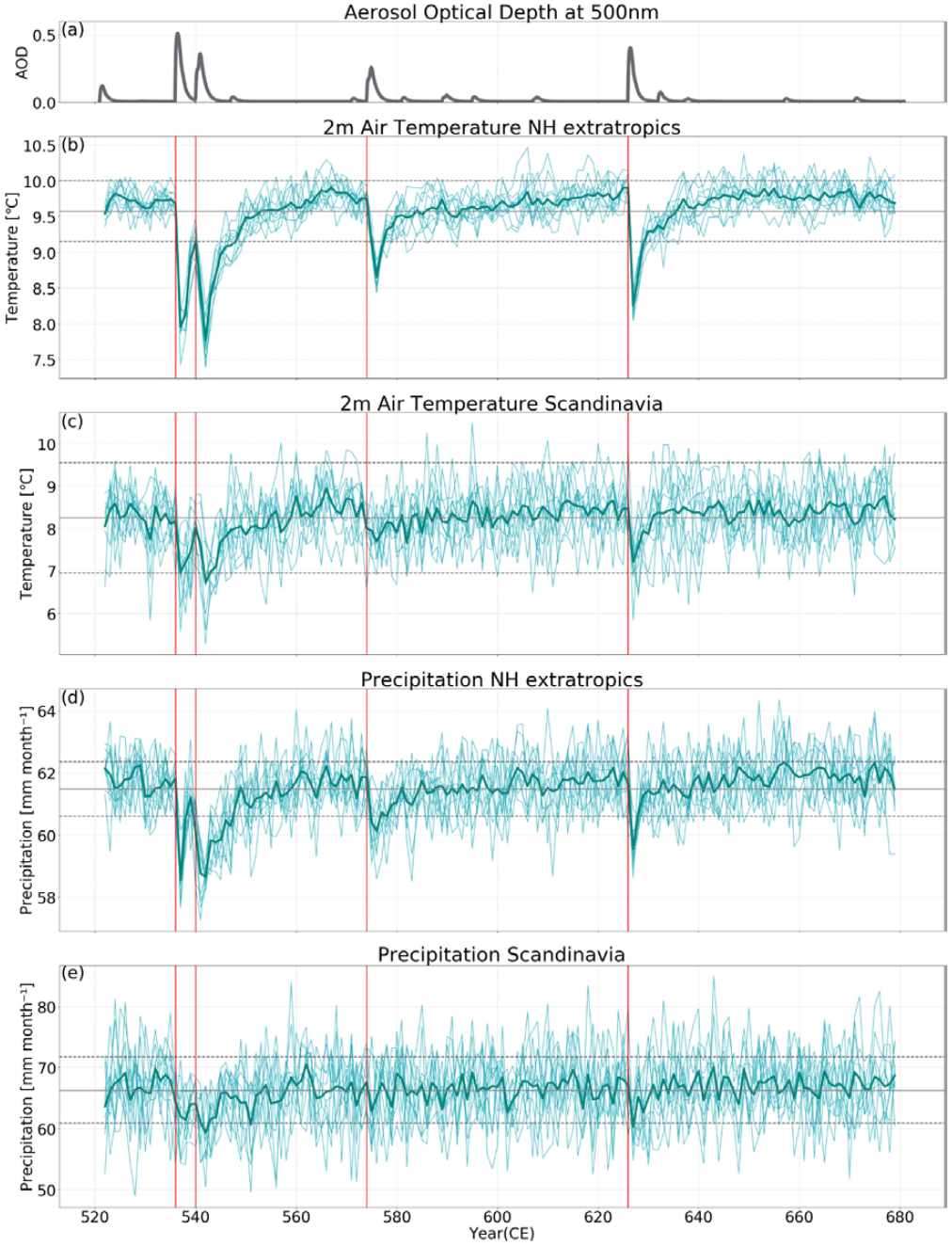

Figure 2. Time series of a) yearly mean NH extratropical (30°-90°N) AOD, and growing season (AMJJAS) mean of b) NH extratropical and c) Scandinavian (0°-20°E, 55°-73°N) 2m air temperature, and d) NH extratropical and e) Scandinavian precipitation. Red vertical lines indicate the four large eruptions in the study period. Grey lines indicate the 0-1850 CE mean and the dashed lines the 1σ (2σ) of the control run for precipitation and (temperature).

https://doi.org/10.5194/cp-2022-23
Preprint. Discussion started: 22 March 2022

The temperature anomaly shows a significant cold period for 25 years after the 536 CE eruption for most of Norway (Fig. 3a), and a significant cooling of up to 2 °C in the first two years after the 536 CE eruption (Fig. 3b) and up to 1.5 °C after the 540 CE eruption (Fig. 3c). Overall, the 5 °Cline shifts south by ~6° in latitude in the first two years after the 536 CE and 540 CE eruptions, covering the northernmost study area site (Fron), where the modelled average growing season temperature drops below 5 °C.

Besides temperature, summer precipitation also impacts the harvest. The ensemble mean indicates that there is a drying during the growing season almost everywhere in Scandinavia, with a significant drying of up to 5 mm month^{-1} 25 years after 536 CE on the 1 σ level (Fig. 3d), and a significant reduction of up to 15 mm month^{-1} (15%) after the 536 CE eruption (Fig. 3e), and up to 20 mm month^{-1} (20 %) in southeastern Norway after the 540 CE eruption (Fig. 3f).

The climate over Scandinavia is influenced by large-scale atmospheric circulation with a dominant positive North Atlantic Oscillation (NAO) circulation pattern during NH winter (Fig. A4a and Section 2.1.2, Michelangeli et al., 1995; Cassou, 2008; van Dijk et al., 2021 in review) and during the growing season (AMJJAS; Fig. A4b). To get a better insight into which circulation patterns are occurring during the growing season after the eruptions, the SLP anomaly is visualised in Fig. 4 for the North Atlantic and Europe region after the 536 CE and 540 CE eruptions. Overall, the large-scale atmospheric circulation pattern reveals a shift to a higher pressure over the high latitudes and a decrease over the mid-latitudes over the North Atlantic region, which corresponds to a reduction of the SLP gradient between the high and low pressure centres. 25 years after the 536 CE, the SLP has slightly and significantly increased over Scandinavia (Fig. 4a). In contrast, the SLP change 2 years after the eruptions is not significant over Scandinavia (Figs. 4b-c).

https://doi.org/10.5194/cp-2022-23
Preprint. Discussion started: 22 March 2022

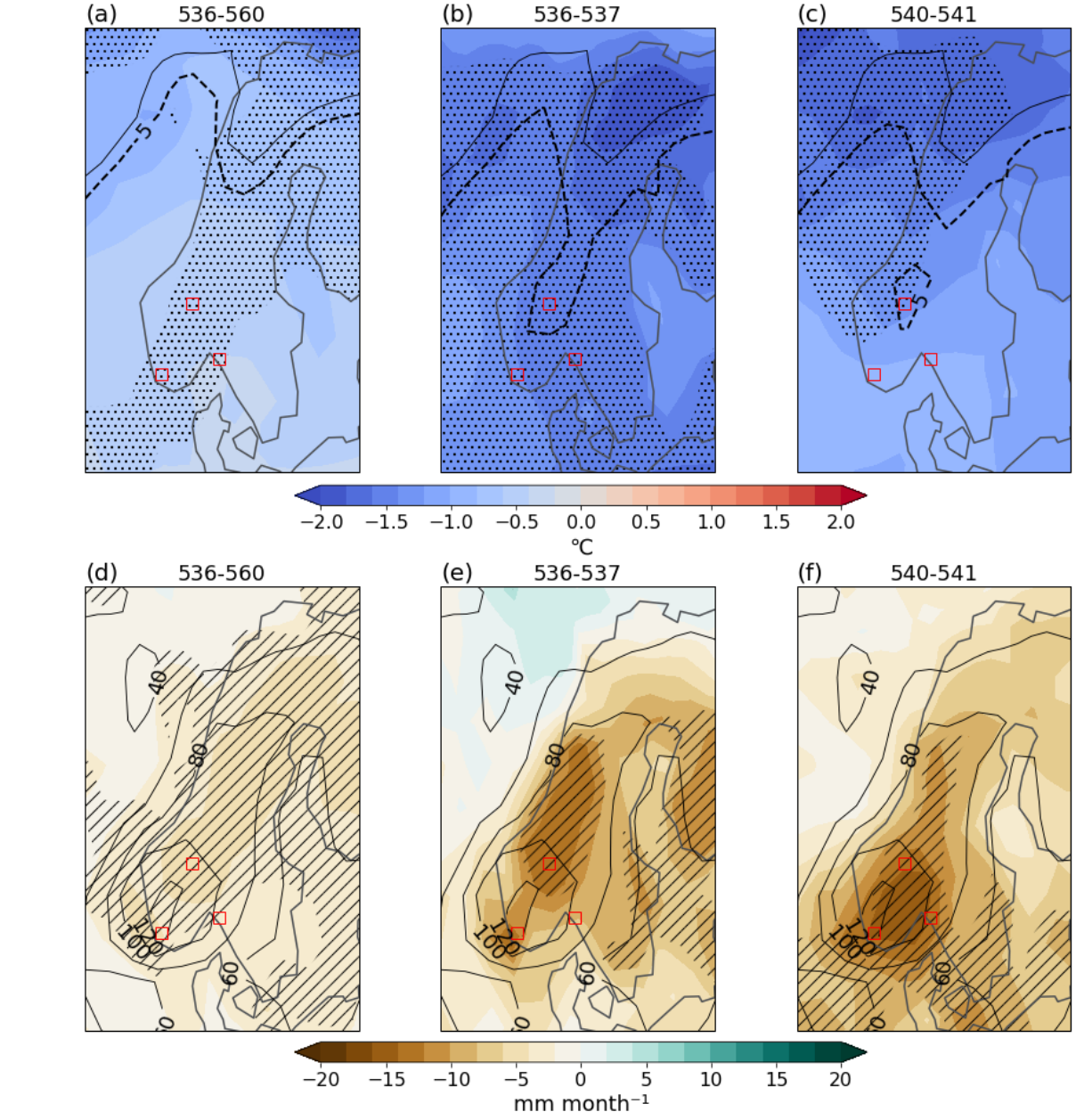

Figure 3. Maps of 2m air temperature (a-c) and precipitation (d-f) anomalies for the mean growing season (AMJJAS) in Scandinavia for 536-560 CE, 536/537 CE, and 540/541 CE. Anomalies are calculated wrt 0-1850 CE. 0-1850 CE climatology in contours. The red squares indicate the locations of the local sites used for the GDD modelling. For temperature, the absolute 5 ℃ line is given by the black dashed and solid contour lines representing the model experiments and climatology respectively. The 1σ (2σ) significant areas are hashed (stippled) for precipitation (2m air temperature).

https://doi.org/10.5194/cp-2022-23
Preprint. Discussion started: 22 March 2022

Climate of the Past Discussions
Open Access
EGU

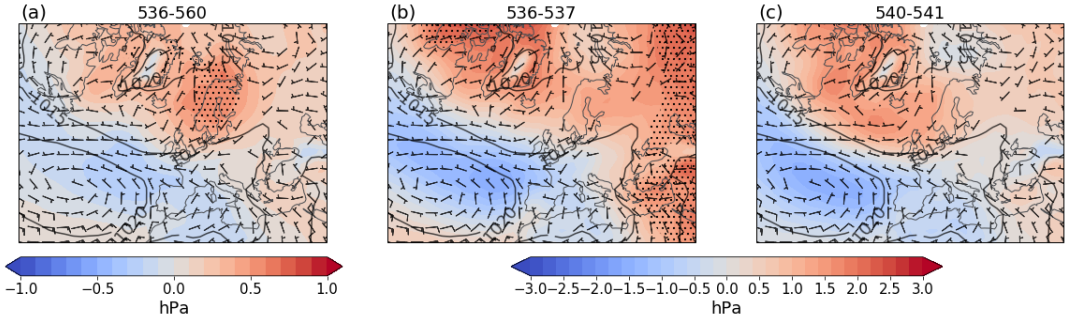

Figure 4. Maps of the North Atlantic ensemble mean sea level pressure anomalies and absolute wind for the mean growing season (AMJJAS) for a) 536-560 CE, b) 536-537 CE, and c) 540-541 CE. Anomalies are calculated wrt 0-1850 CE. 0-1850 CE climatology in contours. The 2σ significant areas are stippled. Wind barbs are shown for 1, 5, and 10 m/s intervals.

As each individual ensemble run is a possible realisation of the modelled volcanic impact, we want to investigate the range of the runs and what the maximum cooling and hydrological effect after the eruptions could be. Interestingly, the temperature anomaly for the 25-year mean growing season reveals a significant cooling from 0.8 to ~1.5 ℃ for half of the runs, whereas the other half shows a non-significant cooling or even a slight warming over Scandinavia (Fig. 5a). Even more striking is, that the 25-year mean precipitation anomaly reveals one ensemble member (ensemble member #3) that shows a significant wetting over south- and northwestern Norway and two members simulating a slight wetting west of Norway (member #5, significant) and over Norway (member #11, non significant), whereas all the other members (9 out of 12) show drying due the surface cooling over the entirety of Scandinavia (Fig. 5b).

Inspecting the first and second growing season after the 536 and 540 CE eruptions (Figs. A1 and A2) further, reveals significant maximum cooling close to 3.6 ℃ for local areas in Norway and a more diverse pattern of wetting and drying over Scandinavia compared to the individual members of the 536-560 CE mean anomalies.

The SLP anomaly maps for the 536-560 CE mean (Fig. 6) reveal eight ensemble members with a significant shift towards higher pressure over the North Atlantic (#5, #7-9, and #12) and Scandinavia (#1-2, and #6), reflecting a weakening of the SLP gradient. The remaining four ensemble members hardly show any significant patterns in atmospheric circulation.

https://doi.org/10.5194/cp-2022-23
Preprint. Discussion started: 22 March 2022

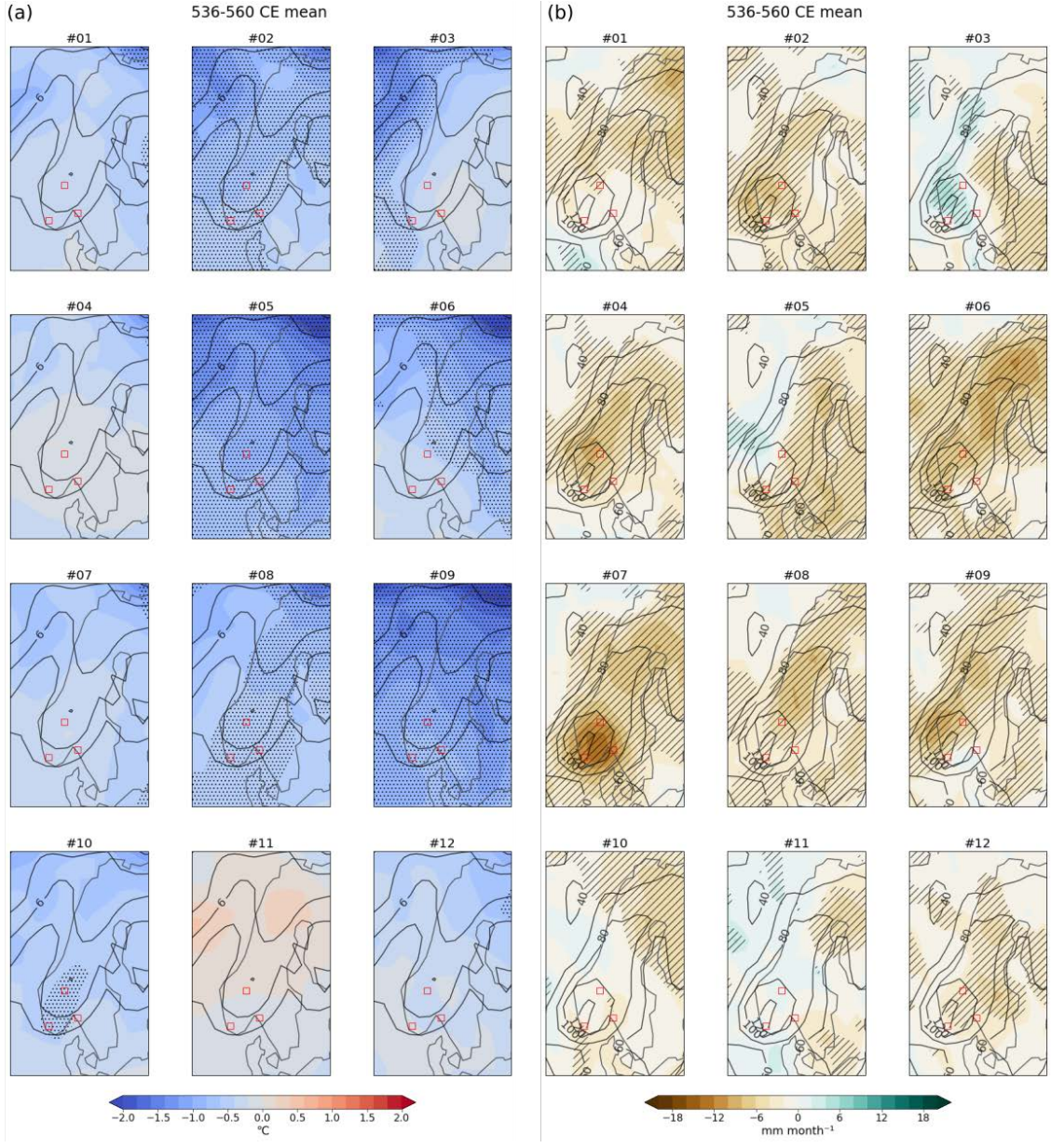

Figure 5. a) temperature and b) precipitation anomaly maps for the mean growing season (536-560 CE) for the individual ensemble members. Anomalies are calculated wrt 0-1850 CE. 0-1850 CE climatology in contours. The red squares indicate the locations of the local sites used for the GDD modelling. The 1σ (2σ) significant areas are hashed (stippled) for precipitation (2m air temperature).

https://doi.org/10.5194/cp-2022-23
Preprint. Discussion started: 22 March 2022

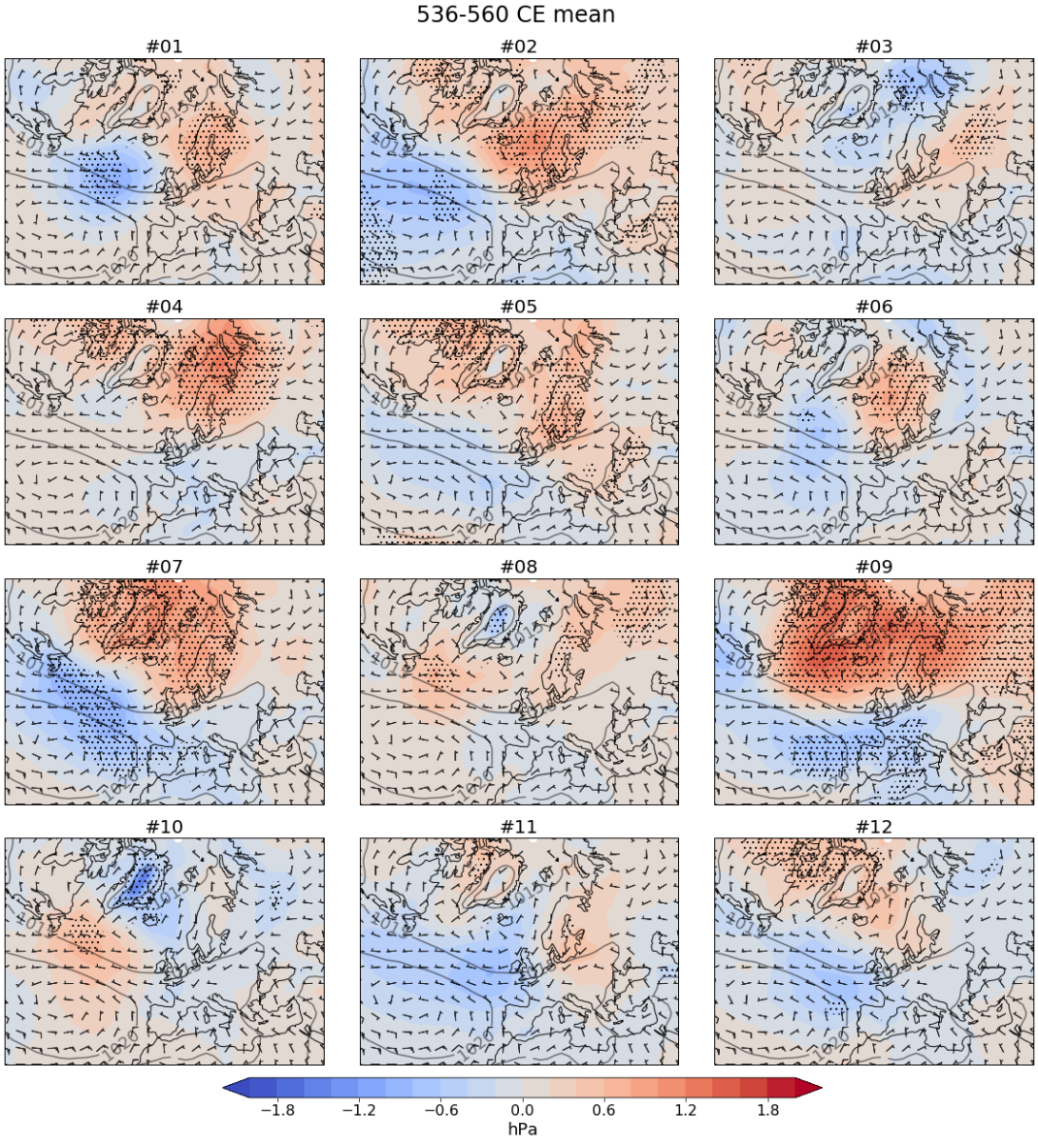

Figure 6. SLP anomaly and absolute 10 m wind maps for the mean growing season for 536-560 CE for the individual ensemble members. Anomalies are calculated wrt 0-1850 CE. 0-1850 CE climatology in contours. The red squares indicate the locations of the local sites used for the GDD modelling. The 2σ significant areas are stippled. Wind barbs are shown for 1, 5 and 10 m/s intervals.

https://doi.org/10.5194/cp-2022-23
Preprint. Discussion started: 22 March 2022


Climate of the Past Discussions
Open Access
EGU

3.2 GDD model results

The average ensemble mean cooling after the 536/540 CE eruptions is 1.6 °C wrt to the 0-1850 mean of the past2k run. Adding the cooling of 0.5 °C wrt to the 1961-1990 mean of the historical run (Table 1) leads to an overall 2.1 °C cooling over Scandinavia. However, individual members reveal a significant maximum cooling after the 536/540 CE up to 3.5 °C over Scandinavia, and a maximum cooling of ~3 °C for Southern Norway (Table 1, Fig. A1). To assess the potential impacts on agriculture for the worst case volcanic climate scenario, we apply a 3 °C cooling in the case study areas for the GDD model set up for 1961-1990 climatological conditions (Fig. 7).

Fron, the northernmost of our case study sites in Southern Norway, is situated in a narrow valley. From the map it becomes clear that with a 3 °C cooling, the accumulated temperature ends up in the 1100-1300 GDD bin for most of the main cultivated area, but with the remaining areas below 1100 GDD. This means that the minimum requirements for crops to grow (Table 2) are only met for rye and barley in the most favourable areas. However, with small margins to account for climate incidents, harvests are likely to fail or be very small even for these species. This area is thus vulnerable to volcanic cooling.

With a 3 °C cooling, the accumulated temperature for Høgsfjorden, located at the southwestern coast of Norway, is around 1400-1700 GDD for the cultivated areas (Figs. 7c,d). This indicates that the minimum requirements are met for rye, barley, and oats, but lower yields can nonetheless be expected for barley and oats. In certain areas, oats may not mature and harvests even fail.

Sarpsborg, located on the eastern side of the Oslo fjord in the southeast of Norway, is a bit warmer than the other two areas, with 1600-1700 accumulated degrees in the growing season after a 3 °C cooling (Figs. 7e-f). Because of low summer precipitation, this means that none of the cereal types appear directly threatened by a cooling event.

https://doi.org/10.5194/cp-2022-23
Preprint. Discussion started: 22 March 2022

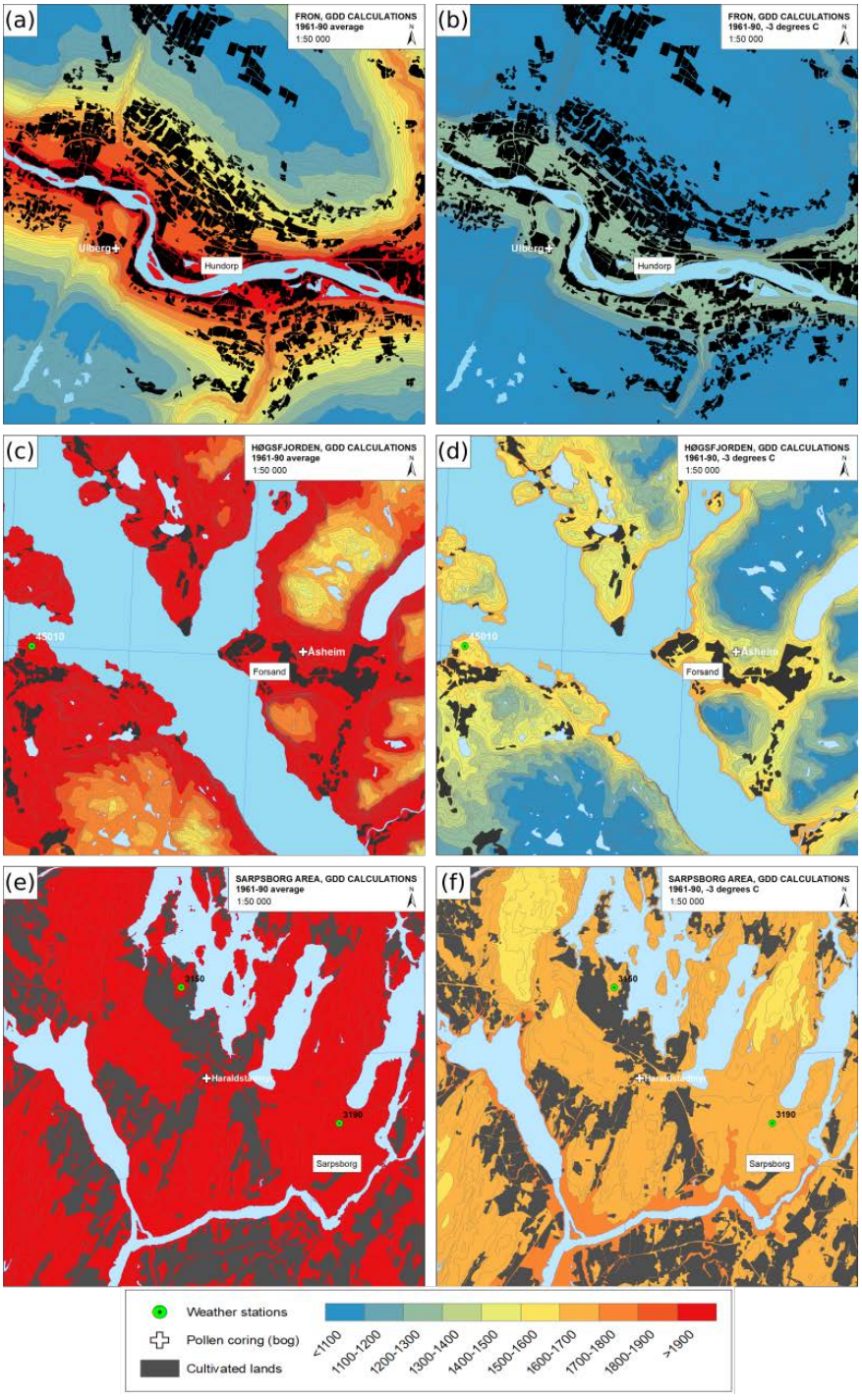

460 **Figure. 7. Growing degree day maps for 1961-1990 for a) Fron, c) Høgsfjorden and e) Sarpsborg and with a 3 °C cooling compared to the 1961-1990 mean for b) Fron, d) Høgsfjorden and f) Sarpsborg.**

https://doi.org/10.5194/cp-2022-23
Preprint. Discussion started: 22 March 2022

3.3 Pollen results

The pollen diagrams (Fig. 8) show the transitions in the vegetation of the three selected area's through time, from ca. 250-1150 CE. The time period from 500-600 CE is marked in each diagram. The total number of pollen (ΣP) is depicted on the uppermost axis. The sum fraction of anthropochores is based on the sum of terrestrial pollen of cultivated taxa that are direct indicators of cultivation (Behre, 1981). These include the four cereals *Secale* (rye), *Avena* (oats), *Triticum* (wheat) and *Hordeum* (barley). The sum fraction of apophytes, plotted on the same axis, is based on the sum of terrestrial pollen of ruderal taxa, which serve as indirect indicators for farming practises; specifically grazing activities (Behre 1981). These include *Rumex* (docks and sorrels), *Rumex longifolius* (northern dock), *Artemisia* (mugwort), *Chenopodiaceae* (goosefoot), *Urtica* (common nettle), *Plantago major* (common plantain) and *Plantago lanceolata* (ribwort plantain). The fungi of *Sordaria* are plotted on a separate axis. Fungi of *Sordaria* can indicate former presence of animals and thus serve as an indicator for grazing activities (van Geel, 2003; Cugny et al., 2010; Etienne et al., 2013; Bajard, 2022). In Figs. A9-A11 extended pollen diagrams are given, outlining the individual taxa of the selected apophytes and trees.

The pollen diagram from the Ulberg bog in the Fron area (Fig. 8a) indicates a decrease in both pollen from the anthropochores taxa as well as pollen from the apophytes taxa during 500-550 CE. Studying the individual species reveals that pollen from *Hordeum* (barley) and *Triticum* (wheat) are less abundant around 500-550 CE, coinciding with a decline in charcoal percentages and an increase in tree pollen. Pollen of *Avena* (oats), in juxtaposition, increase during 500-550 CE. Fungi of *Sordaria* remains absent during this time interval. This 6th century decline is followed by an almost halt to agricultural activities in the 7th century.

In the pollen diagram for Åsheim in the Høgsfjorden area (Fig. 8b), a sharp decline in both the anthropochores and apophytes fractions are noticeable slightly before 550 CE, reaching values down to 0% around 550 CE. This decline is marked by the coinciding disappearance of pollen from *Avena* (oats), *Secale* (rye), *Triticum* (wheat), as well as an absence of fungi from *Sordaria*. Simultaneously, the total number of pollen decreases. After 550 CE, a drop in charcoal and a gradual increase in pollen of trees can be seen. Percentages of *Hordeum* (barley) vary throughout the 6th century, indicating highly irregular cultivation of barley during the entire period.

The pollen diagram for the Haraldstadmyr bog in the Sarpsborg area (Fig. 8c) depicts a slight decline in the sum fractions of anthropochores and apophytes coinciding with an increase in pollen from trees, starting just before 500 CE, followed by a slight and steady increase in the 6th century. From 500-600 CE, the percentages of anthropochores and apophytes remain more or less the same. The pollen for the individual cereals are sparse between 500-600 CE, including a total absence of *Triticum* (wheat) which, however, is not exclusive for this period. Small amounts of *Secale* (rye), *Hordeum* (barley), and *Avena* (oats) remain present. A decrease in charcoal percentages occurs slightly before 550 CE. Overall, less transitions occur between 500-600 CE when compared to the Fron and Høgsfjorden areas.

https://doi.org/10.5194/cp-2022-23
Preprint. Discussion started: 22 March 2022

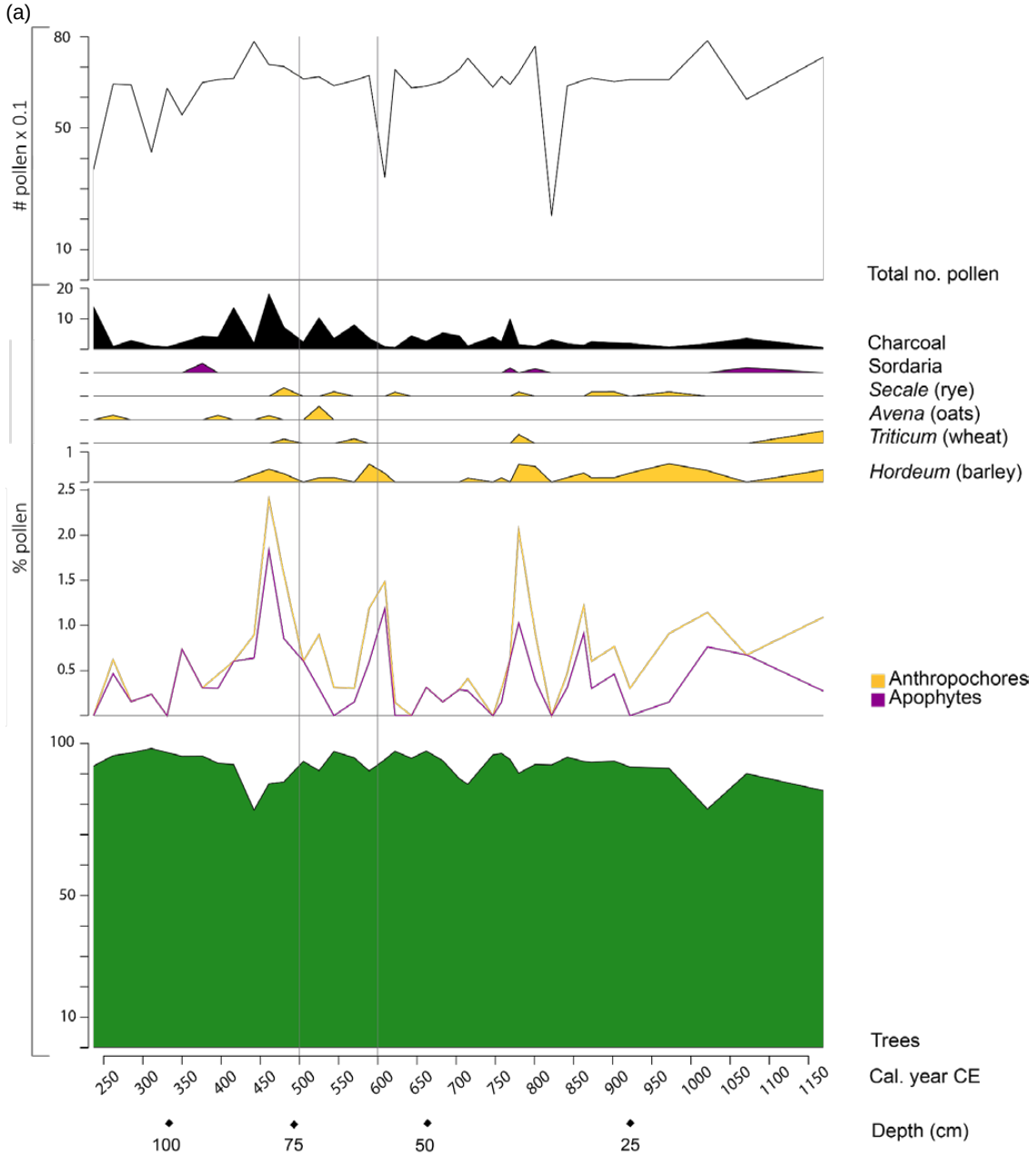

515

https://doi.org/10.5194/cp-2022-23
Preprint. Discussion started: 22 March 2022

520

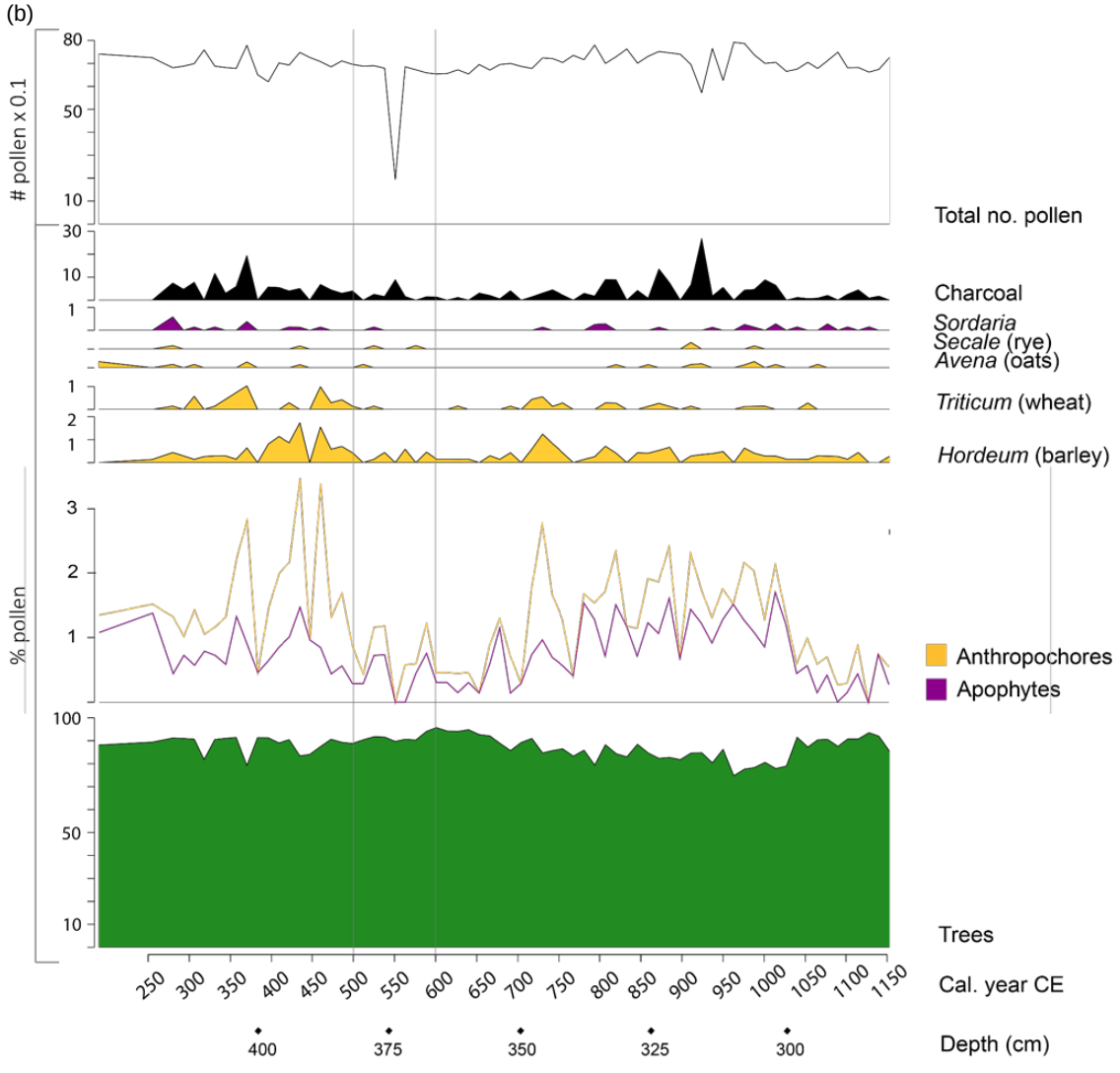

525

530

https://doi.org/10.5194/cp-2022-23
Preprint. Discussion started: 22 March 2022

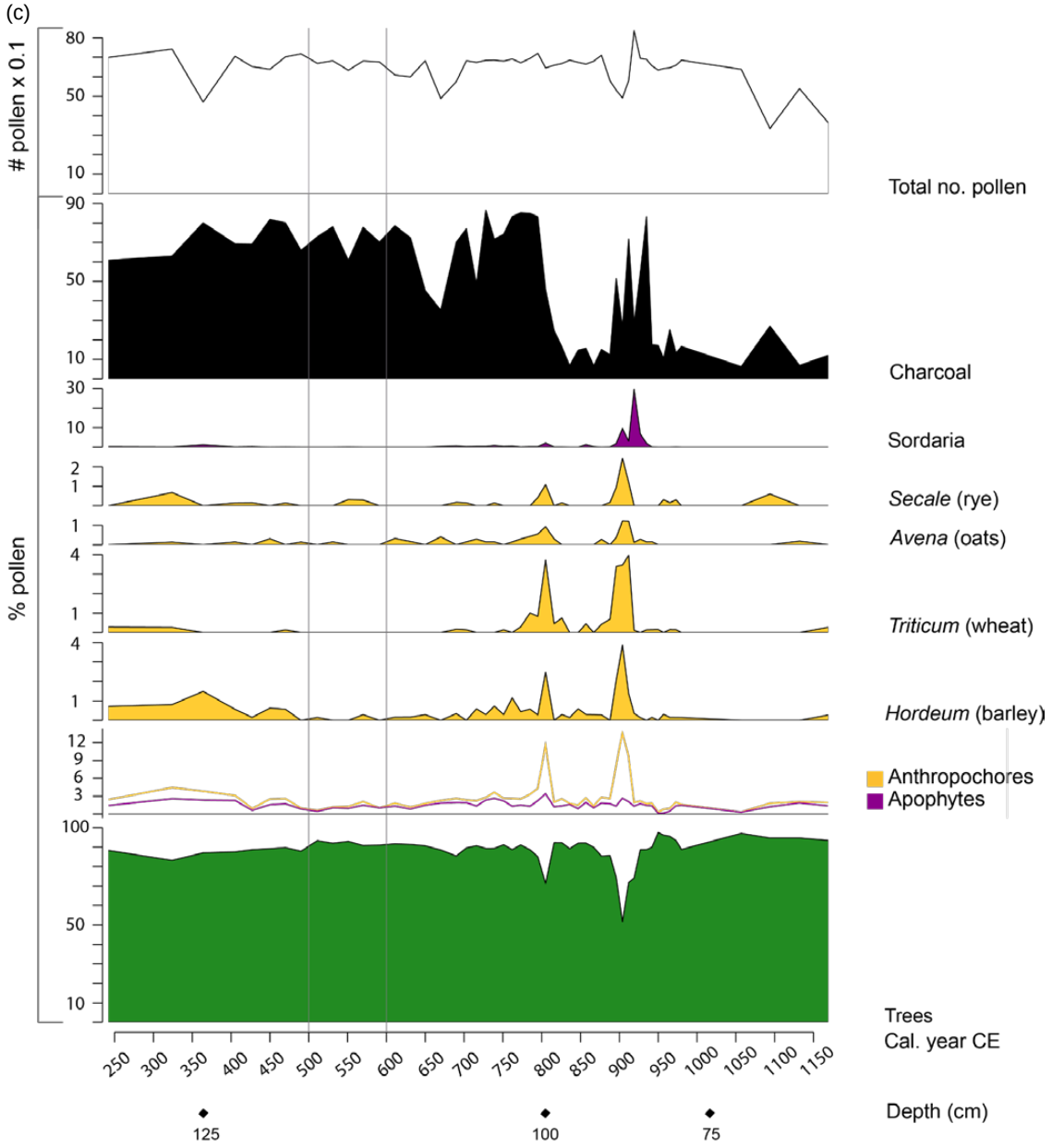

Figure 8. Pollen diagrams for a) Ulberg (Fron area), b) Åsheim (Høgsfjorden area), and c) Haraldstadmyr (Sarpsborg area).

https://doi.org/10.5194/cp-2022-23
Preprint. Discussion started: 22 March 2022

4. Discussion

4.1 Volcanic climate model impact

The mean temperature response for both the short-term and the long-term after the 536/540 CE volcanic double event over Scandinavia is a significant cooling (Fig. 3a). In addition, we simulate a mean growing season of below 5 °C for Fron, which is important for agriculture, as the active growing season is defined as the number of days with temperatures at or above 5 °C. Having an average temperature of 5 °C during the mean growing season (AMJJAS) therefore, could lead to harvest failure, since it is likely that the accumulated temperature sum fails to reach the GDD requirements. For precipitation, the ensemble mean indicates a drying over entire Scandinavia during the 536-560 CE mean as well as for the two years after the eruptions (Fig. 3b). In general, the volcanic induced cooling leads to reduced precipitation/evaporation, as colder air can hold less humidity.

Büntgen et al. (2011) studied the climate variability of the past 2500 years in Europe, and found a reduction in summer temperature due to the volcanic eruptions to coincide with a drying in the sixth-century. Iles and Hegerl (2014) analysed different types of datasets for the most recent eruptions in the period ~1900-2000 CE, and found a drying over Scandinavia in the CMIP5 models, and a drying over Southern Scandinavia as well as wetter conditions over Northern Scandinavia in reanalysis data and data based on satellite and rain gauge observations. Thus, contrasting results have been found on the precipitation response to volcanic eruptions over Scandinavia in previous studies. This is in line with the findings of Tejedor et al. (2021), who studied the global hydroclimate response to large tropical volcanic eruptions using a paleo assimilation product (PHYDA), which uses proxy data in a climate model, as well as an ESM on its own. PHYDA reconstructs a weak signal in the 20 years after all the large (larger than Pinatubo) tropical eruptions in the last millennium, where it seems the west of Scandinavia is getting slightly dryer, and the rest getting slightly wetter. The Old World Drought Atlas (Cook et al., 2015) shows a stronger pattern than PHYDA, with a drying over the southern half of Scandinavia and a wetting in the north, just as the reanalysis and observational data from Iles and Hegerl (2014) suggested. The signal however, is still not very strong (±1.5 on the PDSI scale), which could be due to the averaging over 13 eruptions and taking the 20 year mean. The data sets from Tejedor et al. (2021) represent the soil moisture availability over summer (JJA), and are therefore hard to directly compare to the simulated precipitation response from our climate model simulations. However, together with the precipitation response signal from the other studies, they illustrate that the hydroclimate, including precipitation, is hard to simulate or reconstruct, especially when going further back in time (before the last millennium). Comparing the SLP and precipitation anomaly patterns, and the wind direction, reveals that the precipitation patterns are connected to the atmospheric circulation (Figs. 6, A3).

The atmospheric circulation response after volcanic eruptions for the growing season in Scandinavia has not been studied in detail before. It encompasses the spring to late summer month, which shows a positive like NAO pattern similar as for the NH winter response in the climatology (Fig. A4). After Pinatubo, a positive NAO was observed, which generally leads to warmer and wetter winters in Scandinavia. Climate model simulations from the CMIP3/CMIP4 models however, do not seem to capture this signal (Stenchikov et al., 2002; Driscoll et al., 2012). The summertime atmospheric circulation over the European sector has been studied revealing correlation between the SLP patterns and changes in the North Atlantic storm track (Hurell et al., 2003; Folland et al., 2009). The summertime NAO (SNAO) is defined by Hurell et al. (2003) as a similar mode as the NAO, but with a more confined centre in the Arctic and a more northern high pressure centre over northwestern Europe, for July-August. Zambri et al. (2019) studied the atmospheric circulation patterns for the individual ensemble members after the Laki eruption from 1783-1784, which started in June. They found the temperature response over the North Atlantic sector to be dependent on the atmospheric circulation response. With a

https://doi.org/10.5194/cp-2022-23
Preprint. Discussion started: 22 March 2022

Scandinavian blocking the temperature response is a warming over northwestern Europe and without a blocking they find a cooling over entire Europe and Greenland. This is in line with our findings, where the different circulation responses in the individual ensemble members give different temperature and precipitation anomaly patterns.

From the SLP anomaly in Fig. 4, it can be seen that the atmospheric circulation response over Scandinavia is significant for the ensemble mean growing season for 536-560 CE, but not two years after the 536 CE and 540 CE eruptions. The different patterns in the precipitation and SLP anomalies are cancelled out in the ensemble mean for both the long term and the short term response, resulting in a weak volcanic signal. Even though the 536-560 CE mean gives a significant increase in SLP over Scandinavia (Fig. 4a), the individual runs highlight differences in the regional responses as possible model realisations.

In the two years after the eruptions, the general pattern, like for the long term mean, is that the ensemble members simulating a shift towards higher pressure over Scandinavia also simulate a significant drying over Norway and Sweden accompanied with a reduction in the southwesterly 10 m winds (not shown). However, not all the ensemble members simulate this pattern. For example ensemble member #2 simulates a strong cooling in 537 CE, as well as an increased pressure over Greenland and a decreased pressure over the North Atlantic west of Portugal. This leads to a precipitation pattern with wetter conditions over Western Norway and Central Eastern Sweden. In 541 CE, this member (#2) simulates a significant decrease in pressure over central Europe, leading to dry conditions in Southwestern Norway and wet conditions in Eastern Sweden. This combination of decreased pressure over Europe and a dipole in precipitation over Scandinavia is visible in other members as well (#1 and #12).

Rising water levels in Eastern Swedish lakes and bogs have been reported in our period of interest. During the mid-sixth century, villages in Eastern Central Sweden were abandoned and resettled at higher locations, possibly due to the higher groundwater table (Gräslund and Price, 2012). In Southwest Norway ergot has been discovered at the Forsand excavation site, which indicates wet conditions here as well. A simulation like ensemble member #2, with wetter conditions for both Southwestern Norway and Central Eastern Sweden might therefore be considered as one of the more realistic volcanic climate scenarios.

4.2 GDD model

The GDD requirement numbers in Table 2 are based on experimental studies with traditional cereals in the early 20th century conducted by Foss (1926, 1927). A multitude of local variants existed up to the introduction of standardised farming techniques in the 20th century, and the exact requirements for prehistoric crops are not known. This causes some uncertainty regarding the impact of climate change on Iron Age (500 BCE-1000 CE) farming. The GDD models should therefore be understood as a likely scenario on how volcanic cooling events could have affected Iron Age farming, and as a method for demonstrating differences and similarities for crop cultivation in the three areas.

According to Foss (1926), failing to meet the required temperature sum is by no means directly synonymous with crop failure, but would result in smaller yields and a higher frequency of unripened grains. Unripened grains are unsuited for sowing, and multiple years with low temperatures would thus make it difficult to maintain production. However, unripened grains can still be cut green and used for fodder. A prolonged volcanic cooling, causing multiple years of bad harvests, could therefore lead to necessary changes in subsistence strategies including a shift towards more robust species selection, husbandry practises, and wildlife reliance. Whether this was actually the case must be substantiated by paleo-botanical and archaeological records.

https://doi.org/10.5194/cp-2022-23
Preprint. Discussion started: 22 March 2022

Another issue that should be considered for the GDD modelling is the effect the volcanic aerosols have on the vegetation. There are several historical documents where a dimming of the sun was described, mainly around the Mediterranean area (Stothers, 1984; Rampino et al., 1988). Less sunlight reaching the surface impacts the cultivation of cereals in a negative way by reducing the primary production over several years after the eruptions (Helama et al., 2018). On the other hand, the light following a volcanic eruption is more diffuse, which is known to have a positive impact on plant growth (Fan et al., 2021). However, the GDD model is a simplified model, and here we focus on the temperature, precipitation, altitude, latitude, and growing season length. At the same time, if we would have had the daily data from the climate model, our modelled present-day temperature and GDD estimates could be also off due to the climate model biases and the limited spatial resolution. Therefore, carrying out a scenario with a prescribed volcanic cooling, as we have done here, is more appropriate.

4.3 Pollen record

The pollen record shows a general decrease and low abundance of anthropochores and apophytes, i.e. indicators for human activity, between 500 CE and 600 CE, contemporary with an increase of trees. These findings suggest a decrease in human activity during the 6th century cooling. This decrease is, however, expressed distinctively and to various extents between the different study areas.

The cereals rye, oats, wheat, as direct indicators of cultivation, show a decline for the Høgsfjorden area in the 6th century, indicating crisis and abandonment. This interpretation is strengthened by the coinciding increase in forest. Barley, however, varies to a great extent during the 6th century, implicating a highly irregular cultivation of the cereal throughout this period.
The pollen record from the Sarpsborg area overall displays few transitions for all pollen types, suggesting relatively stable conditions throughout the entire 6th century. The anthropochores and apophytes are relatively scarce in this period, continuing into the 8th century.
In the Fron area, the anthropochores and apophytes show a distinct decline during the 6th century cooling. The individual cereal taxa, however, display inconsistent signals during this period. Pollen from wheat and barley show a decline, whereas pollen from oats show an increase between 500-550 CE. The increase in trees in the Fron area during the 6th century cooling, in combination with the decline in anthropochores and apopythes, is however a strong indicator for crisis and abandonment.

The above pollen analyses have to be interpreted with caution with regard to the calibrated ages used in this study. We have dated 5-9 C14 samples per peat sequence. The C14 ages contain a standard deviation (1σ) varying from 28 to 40 years. In addition, the mean ages in the pollen diagrams are dependent on interpolations made in the age-depth model. The age model could be improved by detecting absolute time markers such as tephra in the bog sediments, which could be part of future work. However, the relative chronology of the transitions in the pollen record with regard to the depth axes remains unaffected by these factors. Other limitations that need to be taken into account include the production-, depositional-, dispersal- and preservation processes of the pollen, which can cause an over- or under-representation of pollen types (Lowe and Walker, 2015).

Various pollen record studies analysing sediment cores in Scandinavia are available covering this period (Høeg, 1996; Høeg, 1997; Wiekowska-Lüth et al., 2017). However, they often span the entire Holocene and are sampled at ~10 cm intervals, giving a temporal resolution of ~120 years. The resolution in the pollen analysis in this study is higher, with sampling intervals of 1-3 cm in the period ~250- 1150 CE, giving a temporal resolution of ~8-24 years. As a result, the more detailed pollen diagrams allow for a more in-depth analysis of shorter time intervals, such as the mid 6th century time period.

https://doi.org/10.5194/cp-2022-23
Preprint. Discussion started: 22 March 2022


Climate of the Past Discussions
Open Access
EGU

4.4 Case study areas

The results for the three case study areas suggest different levels of agricultural vulnerability to a volcanic cooling event, with Fron being particularly vulnerable and Sarpsborg being seemingly resilient towards colder climate conditions. Høgsfjorden is at risk of experiencing reduced harvests, and even crop failure for heat demanding species. Here, we attempt to connect the GDD modelling, pollen analysis and archaeological records to describe possible volcanic climate hazard scenarios for the different areas.

Fron area

Fron is considered a dry area, and is located further north than the other two study areas. The GDD requirements are therefore much lower in Fron than in the other two areas. However, Fron is also associated with a significantly shorter growing season as well as higher altitude. In addition, the landscape is hilly and rugged, which restricts the amount and extension of possible farmlands (Puschmann, 2005).

Three Iron Age farmsteads have been excavated in Fron in 2011-2012. All of them were occupied during the 5th century and subsequently abandoned during the 6th century (Gundersen, 2016, 2021). Their farming strategy was built on a combination of barley cultivation and husbandry.
The pollen record from Fron shows a decrease in anthropochores and apophytes and an increase in trees in the mid 6th century, possibly confirming a short period of abandonment. Some crops, however, such as wheat and barley, sporadically continue to appear in the second half of the 6th century, followed by indications of a temporary halt in farming activity in the 7th century.

In addition, the farms were also situated in areas exposed to floods and landslides, something that seems to have occurred more frequently around the mid-first millennium (Nesje et al., 2016). Around the late 6th or early 7th century, a major flood event buried one of the farmsteads under colluvial sediments, but the archaeological evidence shows that the site was abandoned prior to the flood (Villumsen, 2016). The exact time and character of the site abandonments are somewhat unclear, but seem to have been planned and in response to environmental changes (Gundersen, 2021). The pollen record from nearby Ulberg (Section 4.3) also testifies to a decline and possible halt in crop cultivation around this time. The combined climate model and GDD simulations clearly suggest that the volcanic cooling event could have affected local agriculture in Fron critically, which may have been further disrupted by an increase in flooding rates. However, the lack of widespread settlement excavations in this area makes the scope and consequences of settlement abandonment unclear.

Sarpsborg area

The Sarpsborg area is characterised by relatively high temperatures, a long growing season, and low precipitation (Figs. 1b-c and Table 2). These factors, combined with the presence of wide stretching and fertile agricultural lands (Puschmann, 2005), provide excellent conditions for local agriculture, as well as high resilience against cold summers. The stable conditions for cultivation are reflected in the pollen data from Haraldstadmyr, as relatively few drastic transitions take place in the pollen record from 250 CE to 650 CE.

The area surrounding the Haraldstadmyr bog is characterised by numerous archaeological sites, but only a few of them have been excavated. Important are the recent excavations of a burial site and settlement site at Bjørnstad, situated only 400 metres to the north of Haraldstadmyr (Bårdseth, 2007; Rødsrud, 2007). The settlement site includes a large three-aisled building from around 800 CE that may have included a hall. Another settlement has been excavated at a nearby site at Tune, of what had probably been a farm building from around 400-700 CE (Bårdseth, 2006). The settlement is situated close to a burial site, 600 metres east of Haraldstadmyr, which was excavated in several phases during the 1900s. Characteristic for the Bjørnstad-

https://doi.org/10.5194/cp-2022-23
Preprint. Discussion started: 22 March 2022

Tune sites in the Sarpsborg area is the high percentage of Viking Age burials, which is somewhat in contrast to the rest of former Østfold county (Rødsrud, 2007). There is nonetheless a suspicious lack of Migration Period (400-550 CE) and Merovingian Period (550-800 CE) burials at the Bjørnstad site, which might be indicative of some kind of societal disruption, but with unclear temporal relation to 6th century circumstances. The pollen data indicates a period of slightly reduced farming activities from the mid-5th century to the mid 7th century, namely in the cultivation of cereals. However, due to its early onset, it is uncertain whether this period of reduced farming activities is related to the 6th century circumstances.

Høgsfjorden area

Høgsfjorden has similar temperature conditions as in the Oslofjord area in 1961-1990 (Fig. 7), but also considerably higher precipitation levels (Table 2, Fig. 1b). The large amount of rainfall during the growing season makes it necessary for higher temperatures for the cereals to mature, meaning that the GDD requirements for cereal cultivation are higher than in the Sarpsborg area. The low temperature margins for cultivation makes the Høgsfjorden area susceptible to climate anomalies, which is a more regular feature in the western than the eastern part of Norway.

Large scale excavations have been conducted in the Høgsfjorden area, including a village complex that was continuously occupied from the Bronze Age and up to the 6th century. The site is one of very few settlements of this kind documented in Norway, and consisted in the 5th century of approximately 20 farms (Løken, 2020). However, the 5th century village is also characterised by increasing farming difficulties. Soil exhaustion due to intensive cattle grazing made crop cultivation difficult, leading the farmers to turn to oats cultivation instead of barley and wheat. Oat is a thrifty species and able to grow in poor and less nutritious soils, but is also associated with poor baking qualities and low social status (Bjørnstad, 2012). In addition, it requires a high number of GDD to mature (Table 2). Thus, what may have been a successful adaptation strategy in the 5th century may have increased their vulnerability to the upcoming 6th century cold period. The GDD model for this area suggests that a volcanic cooling event may have negatively affected oats harvests, and potentially caused outright failure. The pollen data confirms this finding, showing a sharp decline in both anthropochores and apophytes in the 6th century cold period, marked by the disappearance of oats, wheat, rye and fungi from *Sordaria.* The archaeological data also include finds of unmatured oats grains and examples of the fungus claviceps purpurea, commonly known as ergot (Løken, 2020). Ergot thrives in a cold and wet climate and infects all sorts of grasses, including grains. It is also highly contagious and the cause for numerous incidents of epidemic ergotism in historical times (Bondeson and Bondesson, 2014). Thus, the archaeological evidence points in the direction of severe social impact from the cooling event, which may have contributed to the final abandonment of the village around 600 CE. However, it should be stressed that continuous settlement occupation has been documented at nearby Forsandneset (Dahl, 2017), and that the abandonment of the village complex is not necessarily expressive for the whole Høgsfjorden area. A recent study of plant macrofossils and pollen data from Rogaland county suggests that rye may have become an important cultivable during the 6th and 7th centuries due to colder climates (Westling and Jensen, 2020).

4.5 Archaeological radiocarbon dates

Radiocarbon datasets are shaped by numerous source-critical issues due to sampling strategies, research priorities, and investigation bias. Settlement sites from the Late Iron Age (c. 550–1000 CE) is for instance underrepresented in the Norwegian archaeological record, thus affecting the number of available C14 dates from this period. The C14 diagrams can therefore not be used as exact expressions for the range and density of past human activities, but is a tool for identifying peaks and troughs in the archaeological record. Whether such anomalies are expressions for research priorities or past settlement activities is a matter of interpretation. In these diagrams, we have excluded the most troubling data – cooking pits and iron production sites – and instead focused on comparable data from throughout the Iron Age (500 BCE-1000 CE). Still, the diagram must

https://doi.org/10.5194/cp-2022-23
Preprint. Discussion started: 22 March 2022


Climate of the Past Discussions
Open Access
EGU

be carefully scrutinised up against research historical issues and how it conditions data representativeness (Loftsgarden and Solheim, in press).

4.5 Synthesis

In this section, we try to bring all the lines of evidence together to sketch a likely scenario of how the volcanic induced cooling could have impacted the local climate and society in Scandinavia. The challenge of this study is to bring together different types of data with different spatial and temporal resolutions, each with their own uncertainties.

The relatively good conditions for agriculture in the Sarpsborg area, even with a volcanic cooling, is in contrast to the conditions for Fron and Høgsfjorden, which are associated with a higher degree of vulnerability. However, the factors contributing to disaster risk in the latter two areas are nonetheless of a different nature. Because of the dry climate and hilly and rugged landscape, the farming landscape in Fron can be understood as marginal compared to the Sarpsborg area. This comparison is, to a certain degree, also valid when it comes to Høgsfjorden, where the mountainous fjord landscapes restrain the farming landscape in similar ways in Fron, but nonetheless including fertile soils and good climate conditions for farming (Puschmann, 2005). The available farmlands in the Høgsfjorden area are therefore extensively cultivated. Flooding remains a considerable challenge for agriculture and settlement in the Gudbrandsdalen valley, while Høgsfjorden is prone to rough weather and high precipitation levels. Thus, although farming in both Fron and Høgsfjorden may be vulnerable to colder conditions, the circumstances are different. Consequently, the course of events leading up to possible harvest failures in the two areas would probably not be identical, and may even be perceived as unrelated by those affected by them. These factors add to the complexity of the potential disaster impact, and how it is experienced in a prehistoric context.

This is also reflected in the pollen data. The apophytes and antropochores in the Fron and Høgsfjorden areas show a clear decline after ~500 CE, coinciding with an increase of forest, whereas this is less evident in the pollen diagram for the Sarpsborg area. Charcoal, however, shows a slight increase in the Fron area between 500-550 CE, as for the Sarpsborg area, and a decline for the Høgsfjorden area. In addition, the pollen record from the Sarpsborg area indicates stable conditions during 500-550 CE, as opposed to turbulent conditions in the Fron and Høgsfjorden areas. Pollen data from other studies indicated a reduction in agriculture in the mid sixth-century in areas in Southern Norway, Sweden and Estonia (Pedersen and Widgren, 2011; Tvauri, 2014; Bajard et al., 2022). However, this is very area dependent. Other archaeological and pollen evidence from southwestern Norway and Sweden shows that not all areas experienced a decline in agriculture (Randheden, 2007; Pedersen and Windgren, 2011).

In addition, for the Høgsfjorden area there is evidence of ergot, indicating wet conditions (Løken, 2020). In eastern Sweden, wet conditions during the period after the 536/540 CE eruptions have also been indicated (Gräslund and Price, 2012). Therefore, climate model ensemble members that simulate wetter conditions rather than a drying together with a pronounced cooling over Scandinavia peak our interest (Figs. A1 and A2). In addition to the evidence for site abandonment from our study areas, archaeological evidence for site abandonment (Solberg, 2000; Löwenborg, 2012) has also been included in our synthesis (Fig. 9). Tree-ring reconstructions from northern Scandinavia (Grudd, 2008; Esper et al., 2012) indicate a cooling of up to 3.5 °C after the 536 CE eruption, which corresponds to the maximum cooling in the model ensemble members (Fig. A1). Figure 9 depicts the above discussed climate and GDD model results, together with archaeological evidence and pollen data for a temperature and precipitation regime that shows a strong cooling, but also wet conditions over Southern Norway and central Sweden. This is by no means the only possibility of the potential climate after the 536/540 CE volcanic double event, but an attempt to visualise several lines of evidence in the form of different types of data sets and methods together. Especially precipitation is highly variable and locally

https://doi.org/10.5194/cp-2022-23
Preprint. Discussion started: 22 March 2022

very different, which makes it hard to reconstruct and/or simulate the past (Iles and Hegerl, 2014; Cook et al., 2015; Tejedor et al., 2021). Thus, higher confidence lies on the cooling after the eruptions, and the consequences this could have on the cultivation of crops and society.

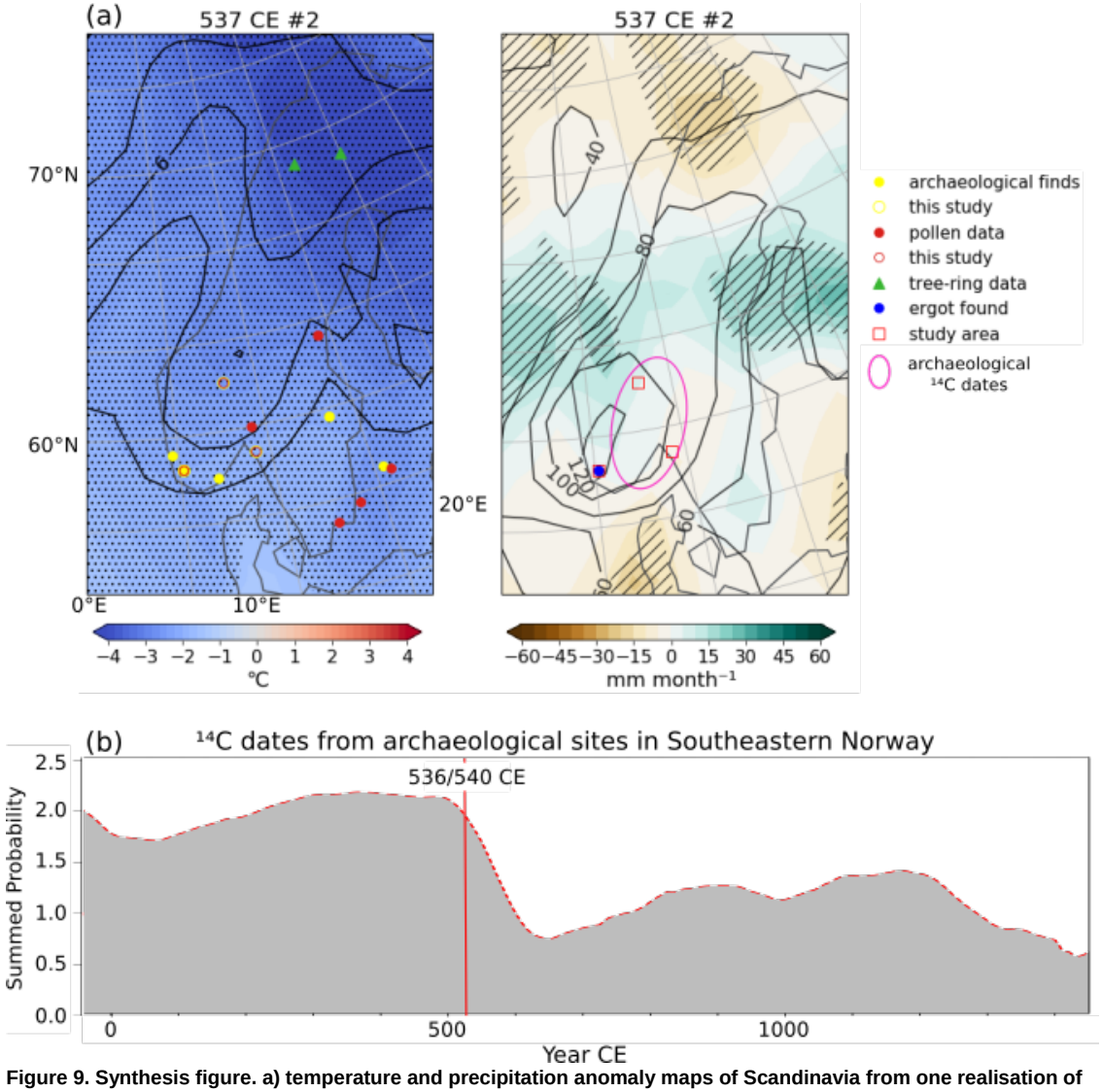

Figure 9. Synthesis figure. a) temperature and precipitation anomaly maps of Scandinavia from one realisation of the MPI-ESM model (ensemble member #2), with markers for archaeological, historical, and pollen proxy data supporting this model simulation. Pollen data showing reduction in agriculture in the mid-500s, archaeological finds indicating abandonment, and tree-ring reconstructions with a 3.5 °C cooling in Northern Scandinavia 1-2 years after the 536 CE eruption. The data used for this figure are listed in Table A4. b) Summed probability distribution of 4012 ¹⁴C dates from archaeological sites in Southeastern Norway (Loftsgarden and Solheim, in press).

https://doi.org/10.5194/cp-2022-23
Preprint. Discussion started: 22 March 2022

5. Conclusion

In this study, we aim to gain more insights into the impacts of the 536/540 CE volcanic double event on the climate and society in Scandinavia, specifically in Southern Norway. Norway's landscape is diverse, with fjords, mountains, valleys, and coasts. This leads to an array of different climate and circulation regimes impacting cultivation practices. Three areas in Southern Norway were selected for a case study, based on different climates and landscapes, and the availability of excavation sites and high-resolution chronological pollen records.

The climate model ensemble mean projects a significant cooling over Scandinavia, and a drying for both the long term 536-560 CE mean as well as for the first two growing seasons after the eruptions 536-537 CE and 540-541 CE. However, individual ensemble members reveal regional differences for the temperature and precipitation anomalies, corresponding to the SLP anomaly patterns. Since the internal climate variability over Scandinavia is high and the model ensemble spread is large, the analysis does not focus on the ensemble mean solely but also inspects individual members as possible volcanic climate impact realisations. For the period after the 536/540 CE volcanic double event, cold and wetter conditions have been indicated by both proxy climate and historical evidence for Southwest Norway and central eastern Sweden, leading to the conclusion that realisations of the climate model ensemble that simulates colder and wetter conditions over these regions may be a more realistic climate model response, though precipitation is highly variable and can be very locally different.

The three selected areas for the case studies reveal from both the GDD model set-up as well as the pollen records, that the areas on the west coast and the mountain areas of Southern Norway experienced a reduction in productivity, and even abandonment of sites in the mid-sixth century, whereas the Oslo fjord area in southeastern Norway showed less indication of crisis during that time. However, the effect on agriculture and society is a complicated picture and the overall impression is one of regionality and varying levels of disaster impact on Iron Age societies. Thus, neither in climatic nor societal terms, the 6th century volcanic induced cooling should be treated as an uniform event throughout Scandinavia. On the contrary, it seems likely that it may have had different consequences throughout the peninsula, thus contributing to considerable regional diversity in human responses to this unique volcanic climate hazard event.

Code and data availability

Primary data and scripts used in the analysis and other supplementary information that may be useful in reproducing the author's work are archived and can be obtained by request. Model results will be available under cera-www.dkrz.de. The PMIP4 past2k simulations contribute to CMIP6 and can be retrieved via the Earth System Grid Federation network (e.g., ttps://esgf-475data.dkrz.de/search/cmip6-dkrz/). Numerous Norwegian archaeological collections as well as almost all surveyed archaeological sites, are digitised and available online (see unimus.no and Askeladden.ra.no)

Author contributions

EvD, IG, and KK conceived the original idea. EvD carried out the climate model runs, processed the data, performed the analysis, and designed the figures for the model and synthesis parts. KK, CT, JJ contributed to the interpretation of the climate model results. IG carried out the GDD model calculations and designed the figures. FI and HH cored the bogs. HH carried out the pollen sampling, -analysis, -counting and 14C sampling. AdB analysed and designed the figures for the pollen data and constructed the age depth models. FI, IG, and KL created the overview map and analysed the archeological sites. KK supervised the research project. All authors discussed the results and helped writing the manuscript.

Competing interests. The authors declare they have no competing interest.

https://doi.org/10.5194/cp-2022-23
Preprint. Discussion started: 22 March 2022

Climate of the Past Discussions

Acknowledgements
This work is funded by the Norwegian Research Council (NFR)/University of Oslo Toppforsk project 'VIKINGS' with the grant number 275191. Computations, analysis and climate model data storage were performed on the computer of the Deutsches Klima Rechenzentrum (DKRZ), and on Sigma2 the National Infrastructure for High Performance Computing and Data Storage in Norway. CT acknowledges support to this research by the Deutsche Forschungsgemeinschaft Research Unit VolImpact (FOR2820,398006378) within the project VolClim (TI 344/2-1). This work also benefited from participation by some authors in the Past Global Changes Volcanic Impacts on Climate and Society working group. We would like to thank Eirik Ballo and Anneke ter Schure for their help with the plotting of the pollen diagrams and the discussion on the age models. Thanks to Robert David for checking the English grammar and spelling.

References

Andersson, T. 2009: Altgermanische Ethnika, Namn och Bygd, 97:5–39.

Axboe, M., 1999. The year 536 and the Scandinavian gold hoards. Medieval Archaeology, 43.

Axboe, M., Capelle, T. and Fischer, C., 2005. Guld og guder. Ragnarok. Odins verden, pp.41-56.

Baillie, M.G., 2008. Proposed re-dating of the European ice core chronology by seven years prior to the 7th century AD. Geophysical Research Letters, 35(15).

Bajard, M., Ballo, E., Høeg, H.I., Bakke, J., Støren, E., Loftsgarden, K., Iversen, F., Hagopian, W., Jahren, A.H., Svensen, H.H. and Krüger, K., 2022. Climate adaptation of pre-Viking societies. Quaternary Science Reviews, 278, p.107374.

Berglund, B.E., Birks, H.J.B., Ralska-Jasiewiczowa, M. and Wright, H.E., 1996. Palaeoecological events during the last 15 000 years. Regional Syntheses of Palaeoecological Studies of Lakes and Mires in Europe. Whiley (Chichester).

Berglund, B.E., 2003. Human impact and climate changes—synchronous events and a causal link?. Quaternary International, 105(1), pp.7-12.

Bjørnstad, Å. 2012. Vårt daglege brød : kornets kulturhistorie (2. utg. ed.). Oslo: Vidarforlaget.

Blaauw, M. and J. A. Christen, 2011. Flexible paleoclimate age-depth models using an autoregressive gamma process. Bayesian Anal 6, 457–474.

Bondeson, L., & Bondesson, T. 2014. On the mystery cloud of AD 536, a crisis in dispute and epidemic ergotism: a linking hypothesis. Danish Journal of Archaeology, 3(1), 61-67. doi:10.1080/21662282.2014.941176

de Bode, A. (2021) 'A pollen-based reconstruction of the paleoenvironment and cultural landscape in Southeastern Norway from the Iron Age to the Middle Ages'. Available at: https://hdl.handle.net/1887/3209493.

Briffa, K.R., Jones, P.D., Schweingruber, F.H. and Osborn, T.J., 1998. Influence of volcanic eruptions on Northern Hemisphere summer temperature over the past 600 years. Nature, 393(6684), pp.450-455.

https://doi.org/10.5194/cp-2022-23
Preprint. Discussion started: 22 March 2022

Brink, S., 2008. Law and society. The Viking World. London: Routledge, pp.23-31.

Brink, S. 2008a: People and land in early Scandinavia. In: P. Geary, P. Urbańczyk and I. H. Garipzanov (eds.): Franks, Northmen, and Slavs: Identities and State Formation in Early Medieval Europe, Cursor Mundi, 5: 87–112. Brepols, Turnhout.

Büntgen, U., Tegel, W., Nicolussi, K., McCormick, M., Frank, D., Trouet, V., Kaplan, J.O., Herzig, F., Heussner, K.U., Wanner, H. and Luterbacher, J., 2011. 2500 years of European climate variability and human susceptibility. science, 331(6017), pp.578-582.

Büntgen, U., Myglan, V.S., Ljungqvist, F.C., McCormick, M., Di Cosmo, N., Sigl, M., Jungclaus, J., Wagner, S., Krusic, P.J., Esper, J. and Kaplan, J.O., 2016. Cooling and societal change during the Late Antique Little Ice Age from 536 to around 660 AD. Nature geoscience, 9(3), pp.231-236.

Bårdseth, G. A. 2006. Huset på Store Tune - og nokre betraktningar om førhistoriske hus i Østfold. In H. Glørstad, B. Skar, & D. Skre (Eds.), Historien i forhistorien. Festskrift til Einar Østmo på 60-årsdagen (pp. 273-280). Oslo: Kulturhistorisk museum, Universitetet i Oslo.

Bårdseth, G. A., Sageider, B. M., & Sandvik, P. U. 2007. Busetjingsspor og mogleg hall frå yngre jarnalder på Bjørnstad søndre (lokalitet 11). In G. A. Bårdseth (Ed.), Hus, gard og graver langs E6 i Sarpsborg kommune. E6-prosjektet Østfold. Band 2 (pp. 71-90). Oslo: Kulturhistorisk museum, Fornminneseksjonen.

Carter, T., R. (1998). Changes in the thermal growing season in Nordic countries during the past century and prospects for the future. Agricultural and Food Science, 7(2), 161-179. doi:10.23986/afsci.72857

Cassou, C., 2008. Intraseasonal interaction between the Madden–Julian oscillation and the North Atlantic Oscillation. Nature, 455(7212), pp.523-527.

Cook, E.R., Seager, R., Kushnir, Y., Briffa, K.R., Büntgen, U., Frank, D., Krusic, P.J., Tegel, W., van der Schrier, G., Andreu-Hayles, L. and Baillie, M., 2015. Old World megadroughts and pluvials during the Common Era. Science advances, 1(10), p.e1500561.

Crema, E.R., Bevan, A. 2020. Inference from large sets of radiocarbon dates: software and methods. Radiocarbon 63(1): 23–39. https://doi.org/10.1017/RDC.2020.95

Dahl, B., Husvegg, J. R., & Åhrberg, E. S. 2017. Arkeologisk og botanisk undersøkelse av hus i Bergevik. Berge gnr. 37 bnr. 1, Forsand kommune, Rogaland. Oppdragsrapport. Unpublished excavation report. Arkeologisk museum, Universitetet i Stavanger.

Degroot, D., Anchukaitis, K., Bauch, M., Burnham, J., Carnegy, F., Cui, J., de Luna, K., Guzowski, P., Hambrecht, G., Huhtamaa, H. and Izdebski, A., 2021. Towards a rigorous understanding of societal responses to climate change. Nature, 591(7851), pp.539-550.

van Dijk, E., Jungclaus, J., Lorenz, S., Timmreck, C. and Krüger, K., 2021. Was there a volcanic induced long lasting cooling over the Northern Hemisphere in the mid 6th–7th century?. Climate of the Past Discussions, pp.1-33.

https://doi.org/10.5194/cp-2022-23
Preprint. Discussion started: 22 March 2022

Driscoll, S., Bozzo, A., Gray, L.J., Robock, A. and Stenchikov, G., 2012. Coupled Model Intercomparison Project 5 (CMIP5) simulations of climate following volcanic eruptions. Journal of Geophysical Research: Atmospheres, 117(D17).

Esper, J., Büntgen, U., Timonen, M. and Frank, D.C., 2012. Variability and extremes of northern Scandinavian summer temperatures over the past two millennia. Global and Planetary Change, 88, pp.1-9.

Fan, Y., Tjiputra, J., Muri, H., Lombardozzi, D., Park, C.E., Wu, S. and Keith, D., 2021. Solar geoengineering can alleviate climate change pressures on crop yields. Nature Food, 2(5), pp.373-381.

Folland, C.K., Knight, J., Linderholm, H.W., Fereday, D., Ineson, S. and Hurrell, J.W., 2009. The summer North Atlantic Oscillation: past, present, and future. Journal of Climate, 22(5), pp.1082-1103.

Foss, H. (1926). Beretning fra Statens forsøksstasjon for fjellbygdene 1925. Ottende arbeidsår. Forsøk med rug og hvete i fjellbygdene. Oslo: Grøndahl & Søns Boktrykkeri.

Foss, H. (1927). Kornavl i fjellbygder. Oslo: Cappelen.

Frøseth, R. B. (2004). Korn. In G. L. Serikstad (Ed.), Økologisk handbok. Matvekster (pp. 167-187). Oslo: GAN Forlag.

Goring, S., Dawson, A., Simpson, G. L., Ram, K., Graham, R. W., Grimm, E. C., and J. W. Williams, 2015. neotoma: A Programmatic Interface to the Neotoma Paleoecological Database. Open Quaternary 1(1), Art. 2. DOI: 10.5334/oq.ab

Gräslund, B. and Price, N., 2012. Twilight of the gods? The 'dust veil event'of AD 536 in critical perspective. Antiquity, 86(332), pp.428-443.

Grudd, H., 2008. Torneträsk tree-ring width and density AD 500–2004: a test of climatic sensitivity and a new 1500-year reconstruction of north Fennoscandian summers. Climate dynamics, 31(7), pp.843-857.

Gundersen, I. M. 2016. Jordbruksbosetninger i dalbunnen. Fellestrekk. In I. M. Gundersen (Ed.), Gård og utmark i Gudbrandsdalen. Arkeologiske undersøkelser i Fron 2011-2012 (pp. 121-130). Kristiansand: Portal forlag.

Gundersen, I. M. 2019. The Fimbulwinter theory and the 6th century crisis in the light of Norwegian archaeology: Towards a human-environmental approach. Primitive tider, 21, pp.101-119.

Gundersen, I. M., Rødsrud, C. L., & Post-Melbye, J. R. 2020: Kokegroper som massemateriale. Regional variasjon i en kulturhistorisk brytningstid. In C. Rødsrud Løchsen & A. Mjærum (Eds.), Ingen vei utenom. Arkeologiske utgravninger i knyttet til etablering av ny riksveg 3 og 25 i Løten og Elverum kommuner, Innlandet (pp. 187-199). Oslo: Cappelen Damm Akademisk forlag.

Gundersen, I. M. 2021. Iron Age Vulnerability. The Fimbulwinter hypothesis and the archaeology of the inlands of eastern Norway. (PhD Monograph). University of Oslo, Oslo.

Hanssen-Bauer, I., Førland, E. J., Haddeland, I., Hisdal, H., Mayer, S., Nesje, A., . . . Ådlandsvik, B. (2017). Climate in Norway 2100 – a knowledge base for climate adaptation(Vol. 1/2017).

https://doi.org/10.5194/cp-2022-23
Preprint. Discussion started: 22 March 2022

Hegerl, G.C., Crowley, T.J., Hyde, W.T. and Frame, D.J., 2006. Climate sensitivity constrained by temperature reconstructions over the past seven centuries. Nature, 440(7087), pp.1029-1032.

Helama, S., Jones, P.D. and Briffa, K.R., 2017. Limited late antique cooling. Nature Geoscience, 10(4), pp.242-243.

Helama, S., Arppe, L., Uusitalo, J., Holopainen, J., Makela, H. M., Makinen, H., . . . Oinonen, M. (2018). Volcanic dust veils from sixth century tree-ring isotopes linked to reduced irradiance, primary production and human health. Sci Rep, 8(1), 1-12. doi:10.1038/s41598-018-19760-w

Hkr = Snorri Sturluson Heimskringla I-II: Old Norse version: Islenzk fornrit, 1941 (1979). Bjarni Agalbjarnarsson (ed.). Reykjavík. Norwegian translation: Heimskringla, utgave Kongesagaer/ Snorre Sturluson (Translated by Anne Holtsmark and Didrik Arup Seip (1979), Norges kongesagaer, 1–2. Oslo.

Høeg, H.I., 1996. Varia 39 Pollenanalytiske undersøkelser i" Østerdalsområdet" med hovedvekt på Rødsmoen, Åmot i Hedmark. Varia http://urn. nb. no/URN: NBN: no-42007.

Høeg, H.I., 1997. Varia 46 Pollenanalytiske undersøkelser på Øvre Romerike, Ullensaker og Nannestad, Akershus kommune. Varia http://urn. nb. no/URN: NBN: no-42007.

Høeg, H. I. 1999. Pollenanalytiske undersøkelser i Rogaland og Ersdal i Vest-Agder. In L. Selsing & G. Lillehammer (Eds.), Museumslandskap. Artikkelsamling til Kerstin Griffin på 60-års-dagen (Vol. AmS-Rapport 12A, pp. 145-225). Stavanger: Arkeologisk museum.

Hines, J. and IJssennagger, N. eds., 2017. Frisians and Their North Sea Neighbours: From the Fifth Century to the Viking Age. Boydell & Brewer.

Hurrell, J.W., 1995. Decadal trends in the North Atlantic Oscillation: Regional temperatures and precipitation. Science, 269(5224), pp.676-679.

Hurrell, J.W., Kushnir, Y., Ottersen, G. and Visbeck, M., 2003. An overview of the North Atlantic oscillation. Geophysical Monograph-American Geophysical Union, 134, pp.1-36.

Indrebø, G.L., 1932. Fylke og fylkesnamn.

Iversen, F. 2016. Estate division: Social cohesion in the aftermath of AD 536-7. In F. Iversen & H. Petersson (Eds.), The Agrarian Life of the North 2000 BC AD 1000: Studies in Rural Settlement and Farming in Norway (pp. 41-76). Kristiansand: Portal Academic.

Iversen, F., 2020. Between Tribe and Kingdom: People, land, and law in Scandia AD 500-1350. Rulership in 1st to 14th century Scandinavia royal graves and sites at Avaldsnes and beyond, Dagfinn Skre (ed.), De Gruter, Berlin, pp.245-304.

Iversen, F. and Brendalsmo, J., 2020. Den tidlige kirkeorganisasjonen i Eidsivatingslagen. Collegium Medievale, 33, pp.113-162.

Iversen, F. (2021). The Four Petty Kingdoms of Upplǫnd: Equestrian Graves and the Political Integration of the Norwegian Highlands in Late Viking Age Norway. Viking, 84(1), 13-42. doi:10.5617/viking.9046

https://doi.org/10.5194/cp-2022-23
Preprint. Discussion started: 22 March 2022

Juggins, S., 2020. rioja: Analysis of Quaternary Science Data. R package version 0.9-26, https://cran.r-project.org/package=rioja.

Jungclaus, J.H., Bard, E., Baroni, M., Braconnot, P., Cao, J., Chini, L.P., Egorova, T., Evans, M., González-Rouco, J.F., Goosse, H. and Hurtt, G.C., 2017. The PMIP4 contribution to CMIP6–Part 3: The last millennium, scientific objective, and experimental design for the PMIP4 past1000 simulations. Geoscientific Model Development, 10(11), pp.4005-4033.

Larsen, L.B., Vinther, B.M., Briffa, K.R., Melvin, T.M., Clausen, H.B., Jones, P.D., Siggaard-Andersen, M.L., Hammer, C.U., Eronen, M., Grudd, H. and Gunnarson, B.E., 2008. New ice core evidence for a volcanic cause of the AD 536 dust veil. Geophysical Research Letters, 35(4).

Little, L.K., 2006. Plague and the end of antiquity: the pandemic of 541-750. Cambridge University Press.

Loftsgarden, K. 2020 Mass production and mountain marketplaces in Norway in the Viking and Middle Ages. Medieval Archaeology 64: 94–115.

Loftsgarden, K. and S. Solheim. In press. Uncovering population dynamics in Southeastearn Norway from 1300 BC to AD 800 using summed radiocarbon probability distributions. In: Ystgaard, I. and M. Ødegaard (Eds.), Complexity and dynamics: Settlement and landscape from the Iron Age and Medieval period in the Nordic Countries. Sidestone Press

Lowe, J.J., Walker, M. and Walker, M.J.C., 2015. Geomorphological evidence. Reconstructing Quaternary Environments: New York, Routledge, pp.19-92.

Løken, T. 2020. Bronze Age and Early Iron Age house and settlement development at Forsandmoen, south-western Norway. Stavanger: Museum of Archaeology, University of Stavanger.

Löwenborg, D., 2012. An Iron Age shock doctrine: did the AD 536-7 event trigger large-scale social changes in the Mälaren valley area?. Journal of Archaeology and Ancient History (JAAH), (4).

Malone, K. 1962: Widsith. Rosenkilde and Bagger, Copenhagen.

Mauritsen, T., Bader, J., Becker, T., Behrens, J., Bittner, M., Brokopf, R., Brovkin, V., Claussen, M., Crueger, T., Esch, M. and Fast, I., 2019. Developments in the MPI-M Earth System Model version 1.2 (MPI-ESM1. 2) and its response to increasing CO2. Journal of Advances in Modeling Earth Systems, 11(4), pp.998-1038.

McCormick, M., Büntgen, U., Cane, M.A., Cook, E.R., Harper, K., Huybers, P., Litt, T., Manning, S.W., Mayewski, P.A., More, A.F. and Nicolussi, K., 2012. Climate change during and after the Roman Empire: reconstructing the past from scientific and historical evidence. Journal of Interdisciplinary History, 43(2), pp.169-220.

McIlveen, J. F. R. (1986). Basic meteorology : a physical outline. Wokingham & Berkshire: Van Nostrand Reinhold UK.

Michelangeli, P.A., Vautard, R. and Legras, B., 1995. Weather regimes: Recurrence and quasi stationarity. Journal of the atmospheric sciences, 52(8), pp.1237-1256.

https://doi.org/10.5194/cp-2022-23
Preprint. Discussion started: 22 March 2022

Miller, G.H., Geirsdóttir, Á., Zhong, Y., Larsen, D.J., Otto-Bliesner, B.L., Holland, M.M., Bailey, D.A., Refsnider, K.A., Lehman, S.J., Southon, J.R. and Anderson, C., 2012. Abrupt onset of the Little Ice Age triggered by volcanism and sustained by sea-ic e/ocean feedbacks. Geophysical Research Letters, 39(2).

Munch, P.A., 1849. Historisk-geographisk beskrivelse over kongeriget Norge (Noregsveldi) i middelalderen. Wilhelm Grams Forlag.

Neidorf, L. 2013: The Dating of Widsith and the Study of Germanic Antiquity. Neophilologus, 97:165–83.

Nesje, A., Gundersen, I. M., & Cannell, R. 2016. Flommer og flomskred i Gudbrandsdalen i et værmessig og klimatisk perspektiv. In I. M. Gundersen (Ed.), Gård og utmark i Gudbrandsdalen. Arkeologiske undersøkelser i Fron 2011-2012 (pp. 80-93). Kristiansand: Portal forlag.

Oinonen, M., Alenius, T., Arppe, L., Bocherens, H., Etu-Sihvola, H., Helama, S., Huhtamaa, H., Lahtinen, M., Mannermaa, K., Onkamo, P. and Palo, J., 2020. Buried in water, burdened by nature—Resilience carried the Iron Age people through Fimbulvinter. PloS one, 15(4), p.e0231787.

Pedersen, E.A., Norseng, P.G. and Stylegar, F.A., 2003. Østfolds historie: Øst for Folden. Bind 1. Østfold fylkeskommune.

Procopius. (1919 [~530-560]). History of the Wars, Volume III (H. B. Dewing, Trans.). In Loeb classical library: Harvard University Press.

Puschmann, O., 2005. Nasjonalt referansesystem for landskap. Beskrivelse av Norges 45 landskapsregioner. NIJOS rapport 10/2005, Ås.

Rampino, M.R., Self, S. and Stothers, R.B., 1988. Volcanic winters. Annual Review of Earth and Planetary Sciences, 16(1), pp.73-99.

Ranheden, H. (2007). Vegetationsförendringar. In E. Hjärthner-Holdar, H. Ranheden, & A. Seiler (Eds.), Land och samhälle i förändring. Uppländska bygder i ett långtidsperspektiv (Vol. vol. 4, pp. 17-118). Uppsala: Riksantikvarieämbetet, Upplandsmuseet, Societas Archaeologica Upsaliensis.

Reimer, P.J., Austin, W.E., Bard, E., Bayliss, A., Blackwell, P.G., Ramsey, C.B., Butzin, M., Cheng, H., Edwards, R.L., Friedrich, M. and Grootes, P.M., 2020. The IntCal20 Northern Hemisphere radiocarbon age calibration curve (0–55 cal kBP). Radiocarbon, 62(4), pp.725-757.

Rosen, W., 2006. Justinian's flea: plague, empire and the birth of Europe. Random House.

Rødsrud Løchsen, C. 2007. Graver og bosetningsspor på Bjørnstad (lokalitet 44). In G. A. Bårdseth (Ed.), Hus, gard og graver langs E6 i Sarpsborg kommune. E6-prosjektet Østfold. Band 2 (pp. 91-183). Oslo: Kulturhistorisk museum, Fornminneseksjonen.

ter Schure, A.T.M., Bajard, M., Loftsgarden, K., Høeg, H.I., Ballo, E., Bakke, J., Støren, E.W.N., Iversen, F., Kool, A., Brysting, A.K. and Krüger, K., 2021. Anthropogenic and environmental drivers of vegetation change in southeastern Norway during the Holocene. Quaternary Science Reviews, 270, p.107175.

Sigl, M., McConnell, J.R., Layman, L., Maselli, O., McGwire, K., Pasteris, D., Dahl-Jensen, D., Steffensen, J.P., Vinther, B., Edwards, R. and Mulvaney, R., 2013. A new bipolar ice core record of volcanism from WAIS

https://doi.org/10.5194/cp-2022-23
Preprint. Discussion started: 22 March 2022

Divide and NEEM and implications for climate forcing of the last 2000 years. Journal of Geophysical Research: Atmospheres, 118(3), pp.1151-1169.

Sigl, M., Winstrup, M., McConnell, J.R., Welten, K.C., Plunkett, G., Ludlow, F., Büntgen, U., Caffee, M., Chellman, N., Dahl-Jensen, D. and Fischer, H., 2015. Timing and climate forcing of volcanic eruptions for the past 2,500 years. Nature, 523(7562), pp.543-549.

Solberg, B., 2006. Signs, symbols and mortuary rituals in the period 200-550/70 AD in Norway. UBAS Nordisk 3. Samfunn, symboler og identitet. Festskrift til Gro Mandt på 70-årsdagen.

Stamnes, A. A. (2016). Effect of temperature change on Iron Age cereal production and settlement patterns in Mid-Norway. In F. Iversen & H. Petersson (Eds.), The Agrarian Life of the North 2000 BC AD 1000 : Studies in Rural Settlement and Farming in Norway (pp. 27-40). Kristiansand: Portal Academic.

Stenchikov, G., Robock, A., Ramaswamy, V., Schwarzkopf, M.D., Hamilton, K. and Ramachandran, S., 2002. Arctic Oscillation response to the 1991 Mount Pinatubo eruption: Effects of volcanic aerosols and ozone depletion. Journal of Geophysical Research: Atmospheres, 107(D24), pp.ACL-28.

Stothers, R.B., 1984. Mystery cloud of AD 536. Nature, 307(5949), pp.344-345.

Strand, E. (1984). Korn og korndyrking. Oslo: Landbruksforlaget.

Sturluson, S. (1963 [~1220-1230]). Kringla heimsins (S. Schjøtt, Trans.). In Kongesoger: Soga om Olav den heilage (Vol. 21). Oslo: Samlaget

TeBrake, W.H., 1978. Ecology and economy in early medieval Frisia. Viator, 9, pp.1-30.

Tejedor, E., Steiger, N.J., Smerdon, J.E., Serrano-Notivoli, R. and Vuille, M., 2021. Global hydroclimatic response to tropical volcanic eruptions over the last millennium. Proceedings of the National Academy of Sciences, 118(12).

Toohey, M., Krüger, K., Sigl, M., Stordal, F. and Svensen, H., 2016. Climatic and societal impacts of a volcanic double event at the dawn of the Middle Ages. Climatic Change, 136(3), pp.401-412.

Tvauri, A., 2014. The impact of the climate catastrophe of 536–537 AD in Estonia and neighbouring areas. Eesti Arheoloogia Ajakiri, 18(1), pp.30-56.

Vautard, R., 1990. Multiple weather regimes over the North Atlantic: Analysis of precursors and successors. Monthly weather review, 118(10), pp.2056-2081.

Verhulst, A., 2002. The carolingian economy. Cambridge University Press.

Villumsen, T. 2016. Jernaldergården på Grytting. Gårdsbosættelse i 500 år i romertid og folkevandringstid. In I. M. Gundersen (Ed.), Gård og utmark i Gudbrandsdalen : arkeologiske undersøkelser i Fron 2011-2012 (pp. 166-180). Kristiansand: Portal forlag.

https://doi.org/10.5194/cp-2022-23
Preprint. Discussion started: 22 March 2022

Welinder, S., 1975. Prehistoric agriculture in Eastern Middle Sweden: a model for food production, population growth, agricultural innovations, and ecological limitations in prehistoric Eastern Middle Sweden 4000 BC-AD 1000 (No. 4). Liberlaromedel.

Westling, S., & Jensen, C. E., 2020. Indications of rye (Secale cereale) cultivation from 7th century south-western Norway. In R. Cappers, W. Kirleis, W. Out, & M. Schepers (Eds.), Archaeobotanical studies of past plant cultivation in northern Europe (pp. 83-100). Groningen: Barkhuis Publishing.

Wickham, H., 2016. ggplot2: elegant graphics for data analysis. springer.

Wickham, H., Averick, M., Bryan, J., Chang, W., McGowan, L.D.A., François, R., Grolemund, G., Hayes, A., Henry, L., Hester, J. and Kuhn, M., 2019. Welcome to the Tidyverse. Journal of open source software, 4(43), p.1686.

Wieckowska-Lüth, M., Kirleis, W. and Doerfler, W., 2017. Holocene history of landscape development in the catchment of Lake Skogstjern, southeastern Norway, based on a high-resolution multi-proxy record. The Holocene, 27(12), pp.1928-1947.

Zambri, B., Robock, A., Mills, M.J. and Schmidt, A., 2019. Modeling the 1783–1784 Laki eruption in Iceland: 2. Climate impacts. Journal of Geophysical Research: Atmospheres, 124(13), pp.6770-6790.

Zhong, Y., Miller, G.H., Otto-Bliesner, B.L., Holland, M.M., Bailey, D.A., Schneider, D.P. and Geirsdottir, A., 2011. Centennial-scale climate change from decadally-paced explosive volcanism: a coupled sea ice-ocean mechanism. Climate Dynamics, 37(11), pp.2373-2387.

Åssveen, M., & Abrahamsen, U. (1999). Varmesum for sorter og arter av korn. Grønn forskning(2), 55-59.

https://doi.org/10.5194/cp-2022-23
Preprint. Discussion started: 22 March 2022

Climate of the Past Discussions

Appendix A - Climate model simulations

1250

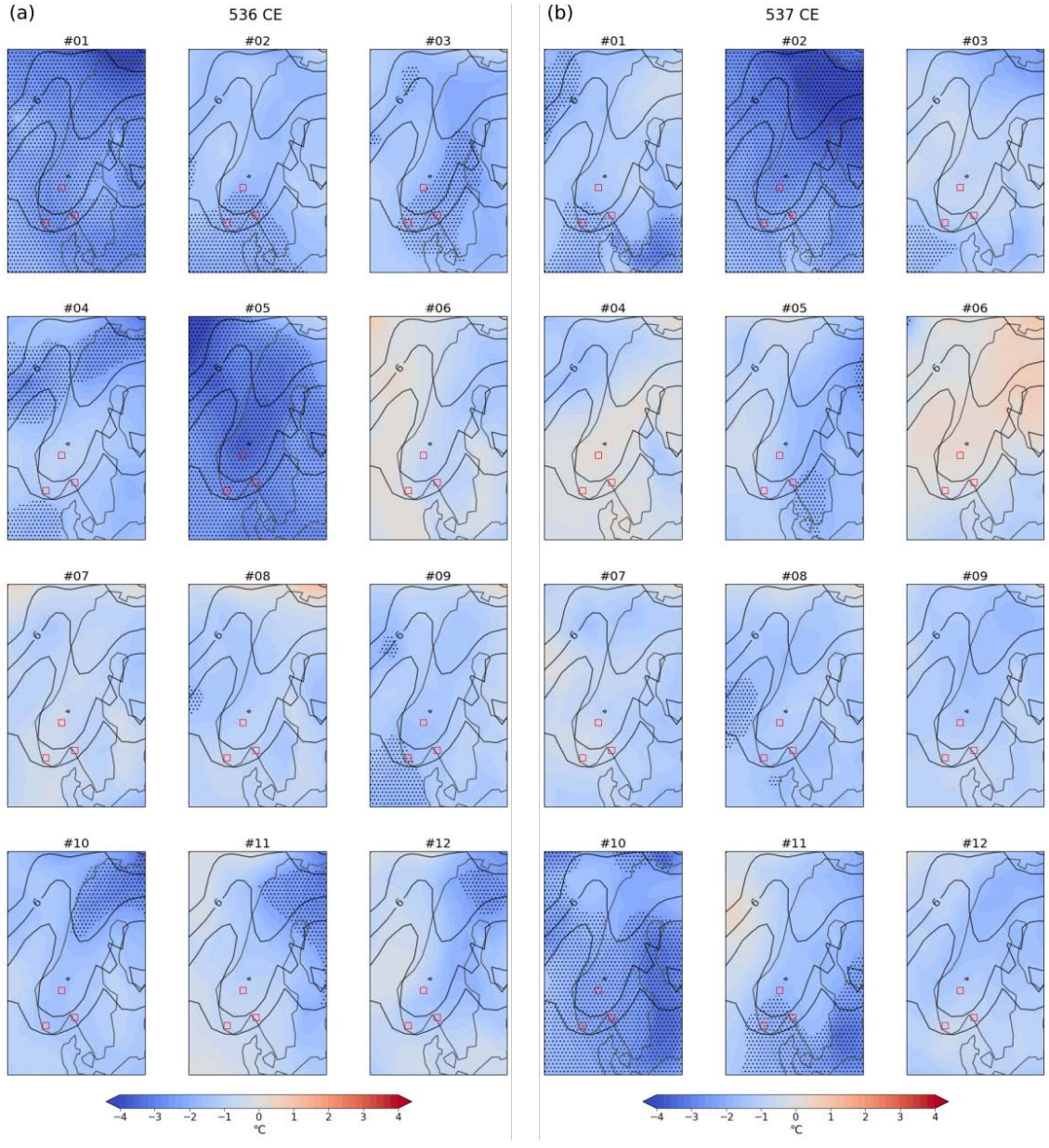

https://doi.org/10.5194/cp-2022-23
Preprint. Discussion started: 22 March 2022

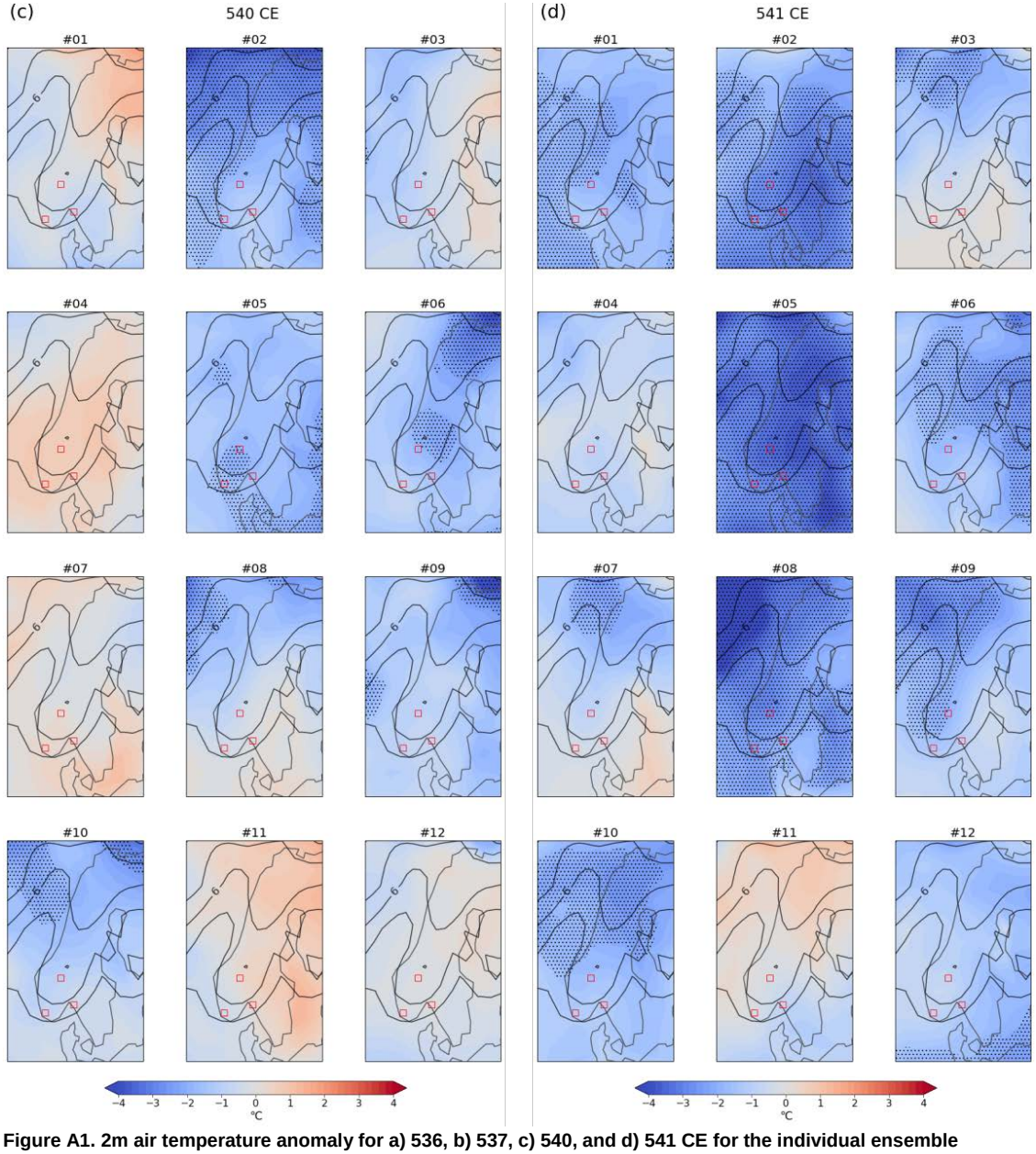

Figure A1. 2m air temperature anomaly for a) 536, b) 537, c) 540, and d) 541 CE for the individual ensemble members. Anomalies are calculated wrt 0-1850 CE. 0-1850 CE climatology in contours. The red squares indicate the areas used for growing degree day calculations. The 2σ significant level is stippled.

https://doi.org/10.5194/cp-2022-23
Preprint. Discussion started: 22 March 2022

Climate of the Past Discussions
Open Access
EGU

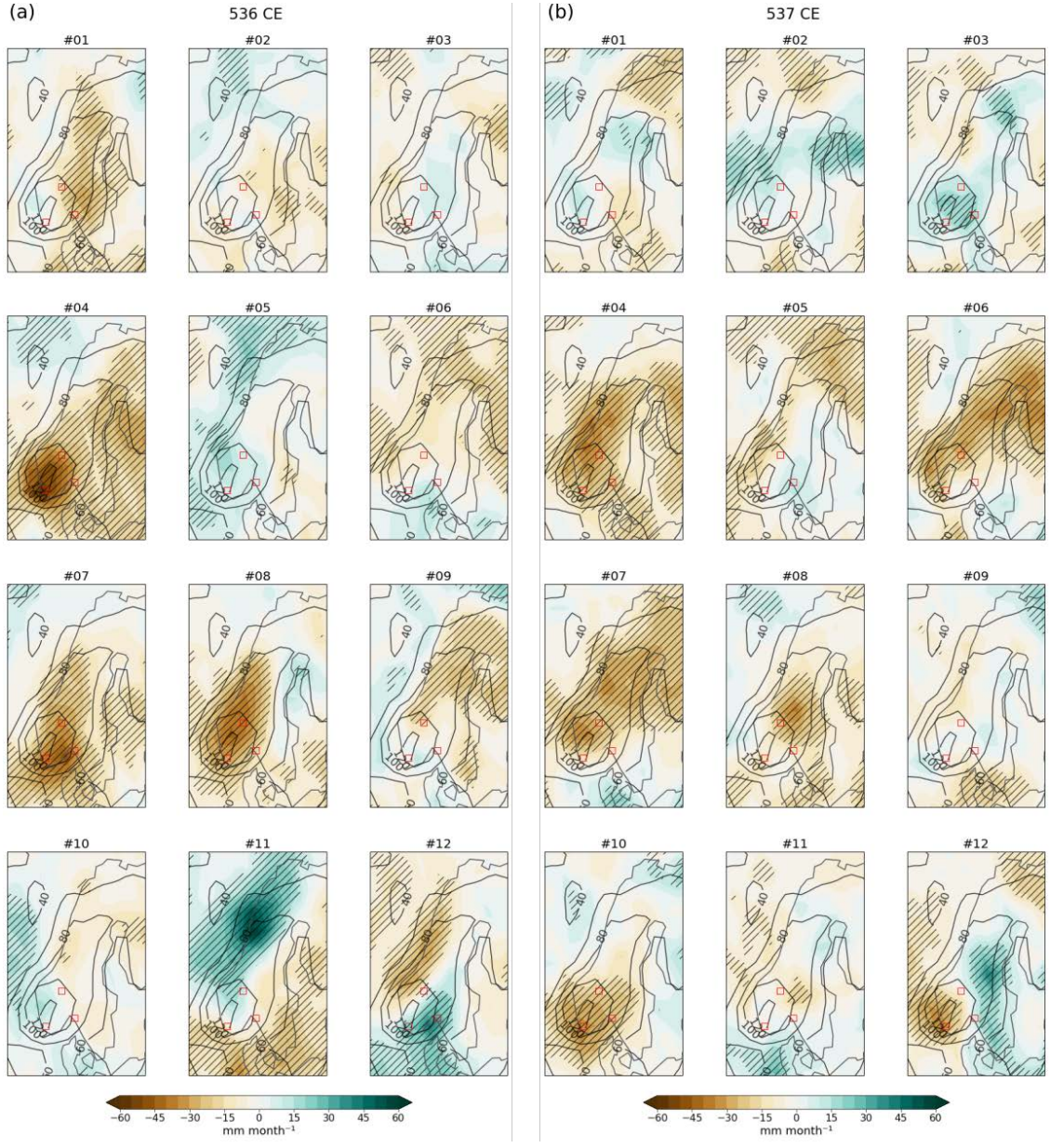

https://doi.org/10.5194/cp-2022-23
Preprint. Discussion started: 22 March 2022

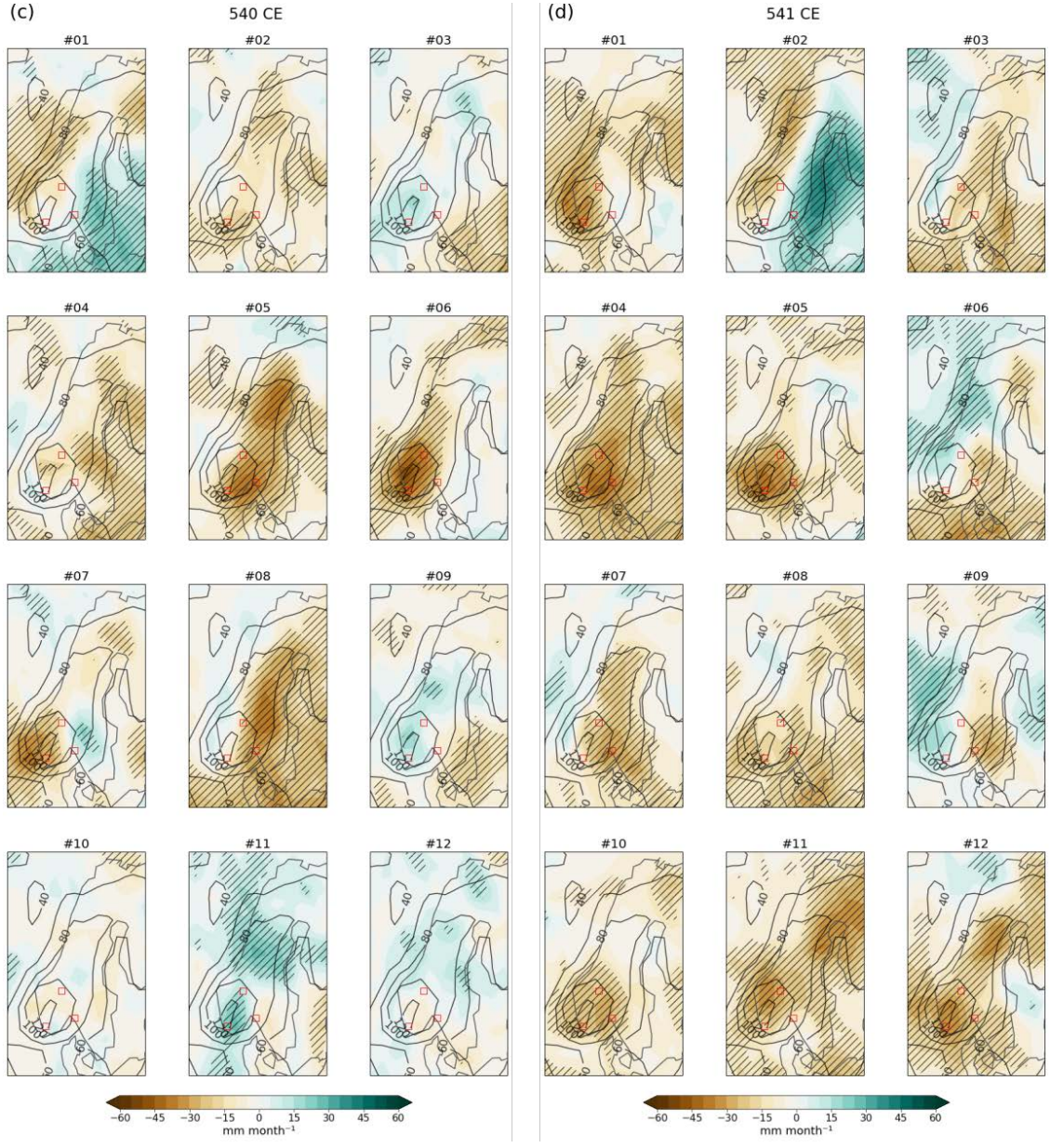

Figure A2. Precipitation anomaly for the mean growing season in a) 536, b) 537, c) 540 and d) 541 CE for the individual ensemble members. Anomalies are calculated wrt 0-1850 CE. 0-1850 CE climatology in contours. The red squares indicate the growing degree day areas. The 1σ significant areas are hatched.

https://doi.org/10.5194/cp-2022-23
Preprint. Discussion started: 22 March 2022

Climate of the Past Discussions
Open Access
EGU

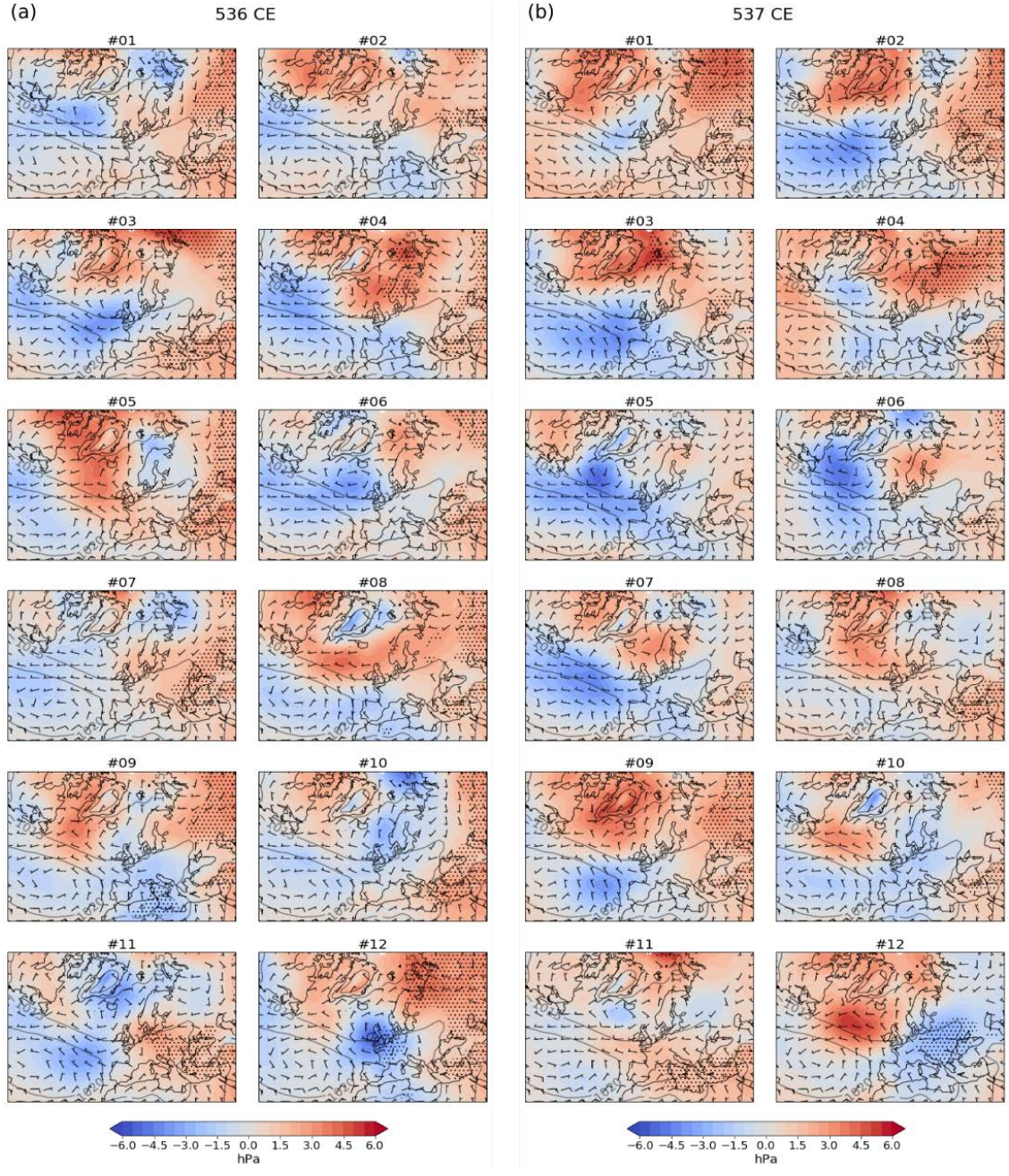

https://doi.org/10.5194/cp-2022-23
Preprint. Discussion started: 22 March 2022

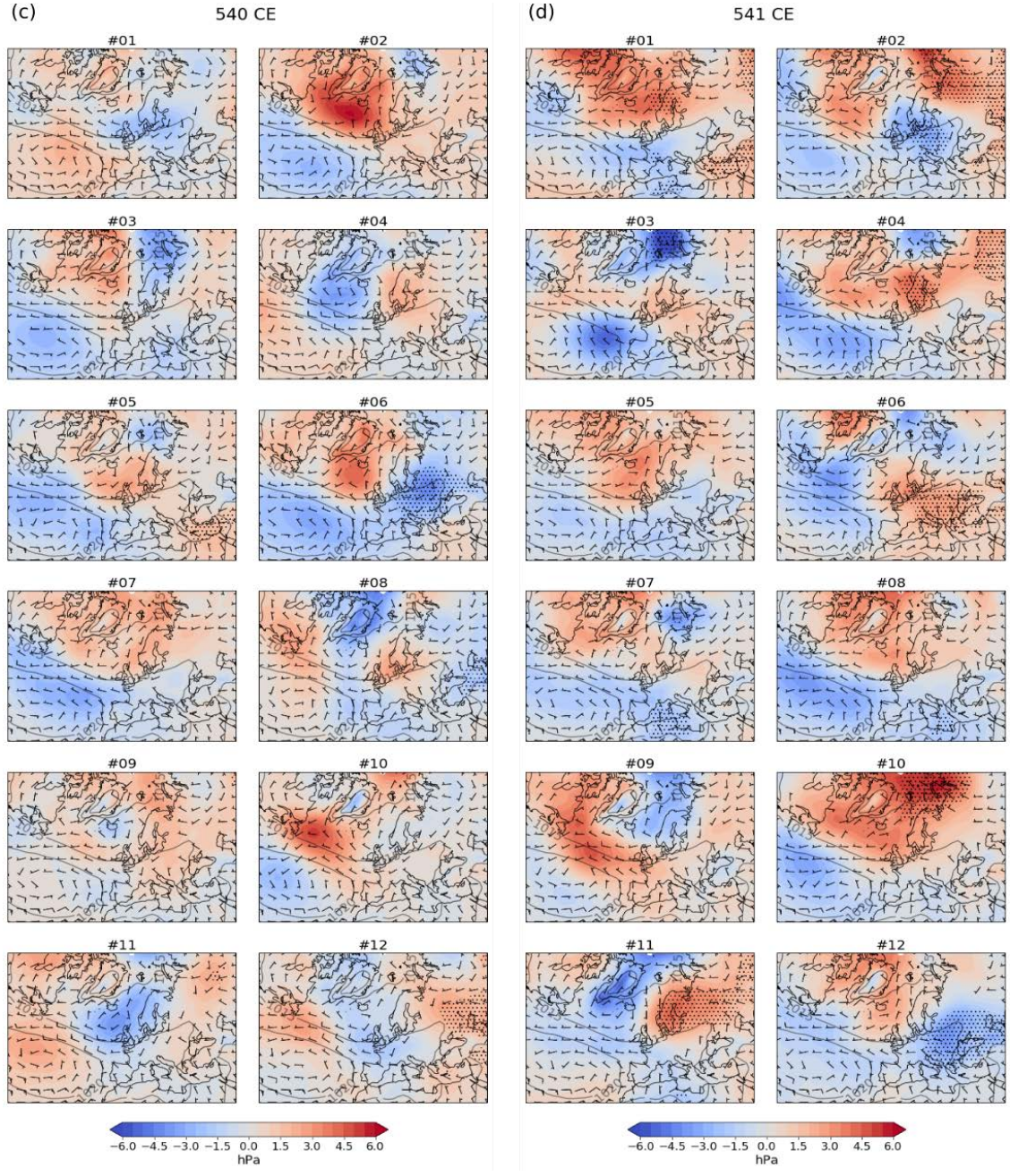

Figure A3. Sea level pressure anomaly and absolute wind for the mean growing season in a) 536, b) 537, c) 540 and d) 541 CE for the individual ensemble members. Anomalies are calculated wrt 0-1850 CE. 0-1850 CE climatology in contours. The 2σ significant areas are stippled. Wind barbs are shown for 1, 5 and 10 m/s intervals.

Analysing the general atmospheric circulation patterns by using EOF analysis, for the April-September growing season from the past2k run #1 (Fig. A4b), reveals the growing season atmospheric circulation anomaly

https://doi.org/10.5194/cp-2022-23
Preprint. Discussion started: 22 March 2022

patterns to be a combination of the winter and summer modes (not shown here), with a similar distribution of high and low pressure centres as in winter, but not as concentrated. The four leading modes are a NAO+ like pattern with 38%, a NAO- like pattern with 8%, a weaker NAO+ like pattern with 7% and a blocking like pattern with the high pressure over the Kara sea with 6%.

Van Dijk et al. (2021 in review) show a significant SLP anomaly, with an increase over the high latitudes and a decrease over the mid-latitudes two years after the large eruptions that occurred during 520-680 CE for JJA, whereas the DJF signal is not significant due to high internal variability in the winter months. These SLP patterns are similar as we find in this study for the mean growing season (Fig. 4), with a higher pressure over the high latitudes and land, and a decrease in pressure over the mid-latitudes for the NH. In addition, van Dijk et al. (2021, in review) calculated the NAO index for the DJF SLP, resulting in a positive NAO response the first year after the eruption for three out of four eruptions, followed by a more neutral or even a negative NAO response in the year after.

From the SLP anomaly in Fig. 4, it can be seen that the atmospheric circulation response over Scandinavia is significant for the ensemble mean growing season for 536-560 CE, but not two years after the 536 and 540 eruptions. The different patterns in the precipitation and SLP anomalies are cancelled out in the ensemble mean, resulting in a weak volcanic signal. Even though the 536-560 CE mean gives a significant anomaly for Scandinavia (Fig. 4a), the individual runs highlight differences in the regional responses as possible realisations.

https://doi.org/10.5194/cp-2022-23
Preprint. Discussion started: 22 March 2022

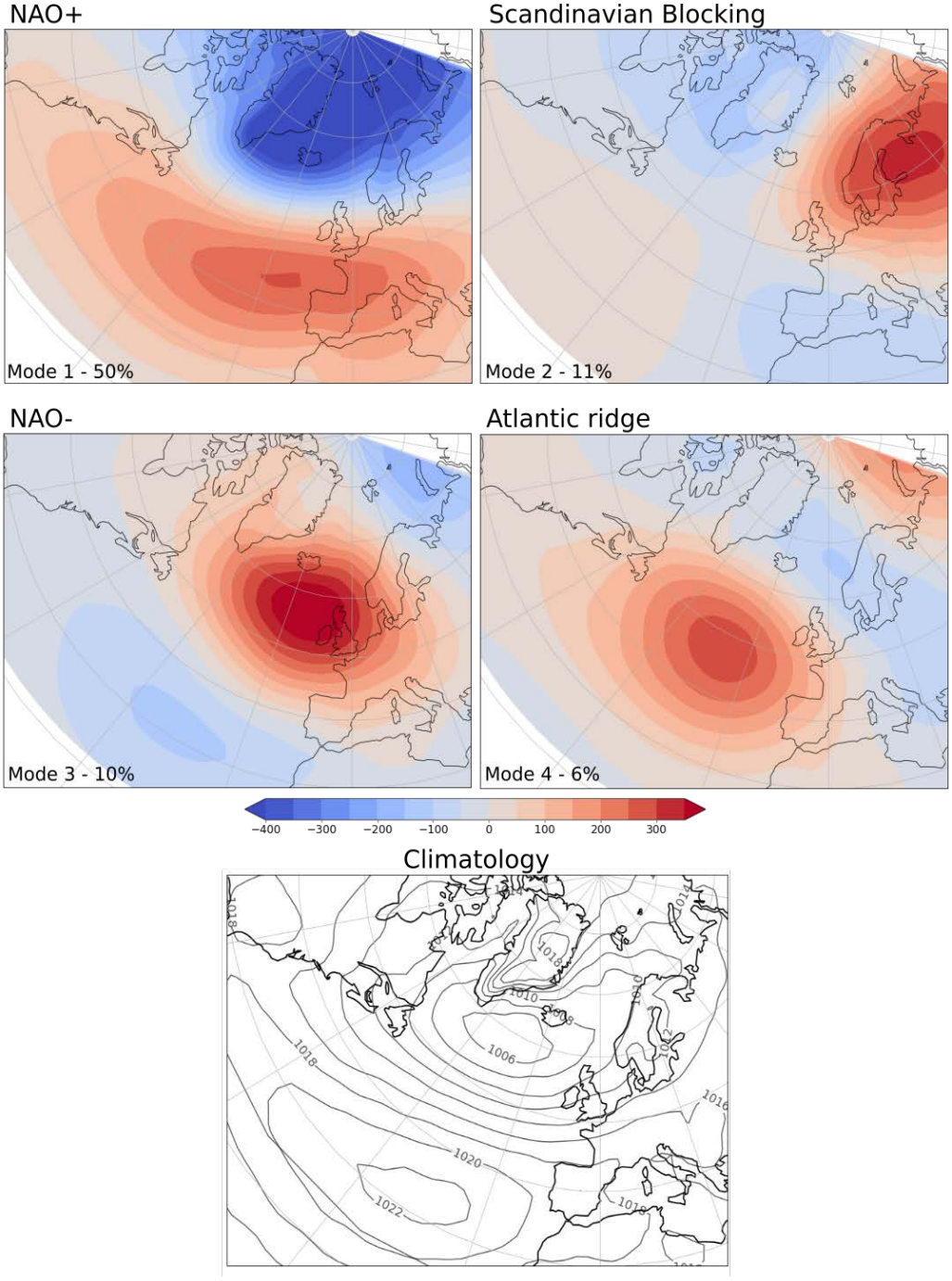

https://doi.org/10.5194/cp-2022-23
Preprint. Discussion started: 22 March 2022

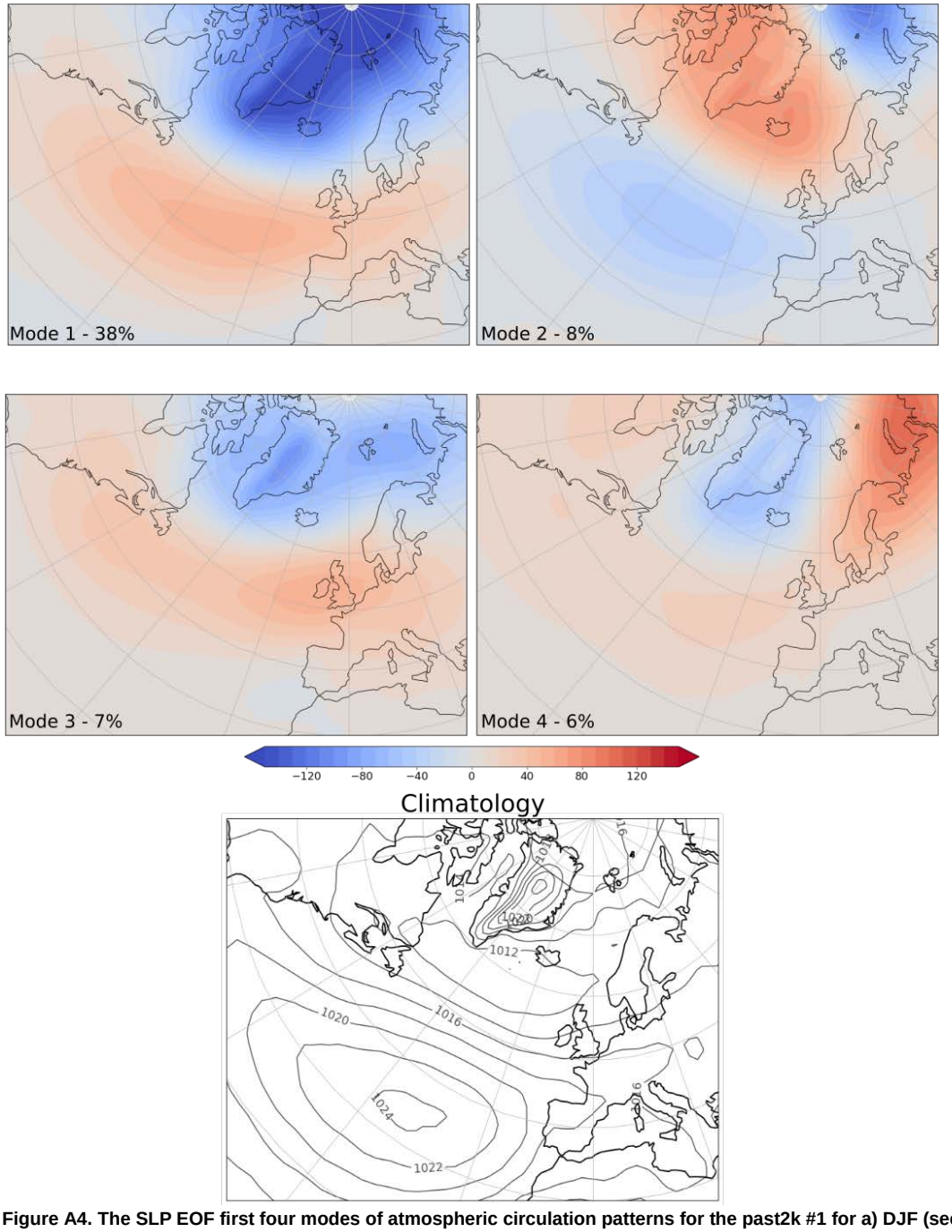

Figure A4. The SLP EOF first four modes of atmospheric circulation patterns for the past2k #1 for a) DJF (see also van Dijk et al., 2021 in review) and b) the mean growing season (AMJJAS) during 0-1850 CE. The SLP climatology for 0-1850 CE is given in the lowest panel; contours are given in 2 hPa intervals.

Appendix B - Study sites

https://doi.org/10.5194/cp-2022-23
Preprint. Discussion started: 22 March 2022

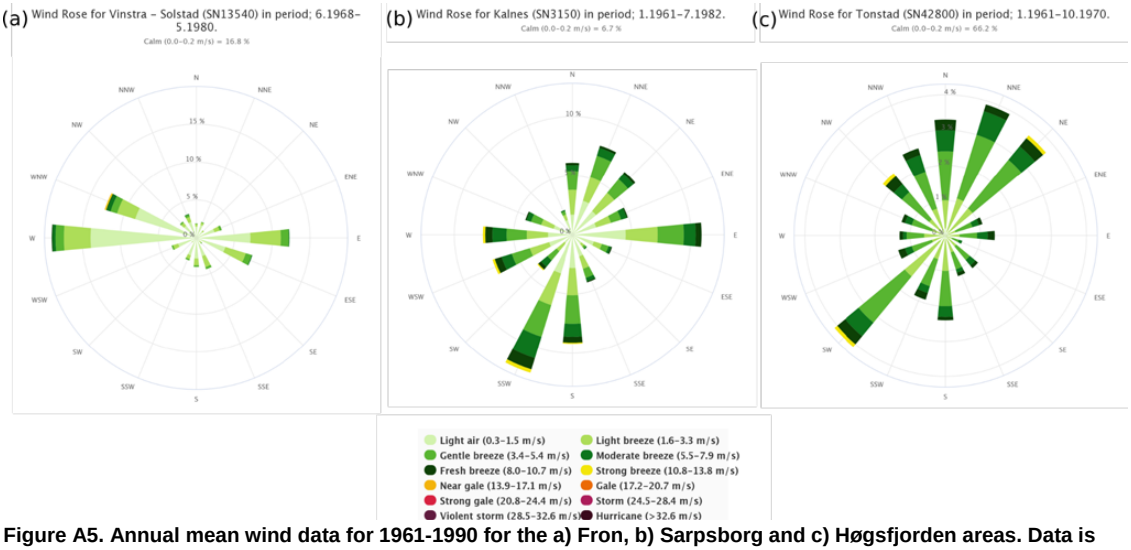

Figure A5. Annual mean wind data for 1961-1990 for the a) Fron, b) Sarpsborg and c) Høgsfjorden areas. Data is taken from the nearest meteorological station with the same valley orientation as the study area.

Appendix C - Pollen data

Chronology

The uncalibrated and calibrated radiocarbon ages of Haraldstadmyr peat sequence are presented in Table A1. An age-depth model was generated based on these 9 radiocarbon ages, as presented in Fig. A6. The top of the core, i.e. 0 cm, was incorporated in the construction of the age-depth model as the year of the coring, i.e. 2018 CE.

The age-depth model indicates that the peat sequence approximately covers the last 4000 years. The peat accumulations vary throughout the core. From 0-45 cm, the accumulation rate measures 0.36 mm/yr. The accumulation rate increases from 45-109.5 cm to 1.18 mm/yr. From 109.5-275.5 cm, the mean accumulation rate measures 0.52 mm/yr.

Table A1: Radiocarbon ages for Haraldstadmyr peat sequence.

https://doi.org/10.5194/cp-2022-23
Preprint. Discussion started: 22 March 2022

Lab number	Core depth (cm)	^{14}C age BP	Min. age (cal BP)	Max. age (cal BP)	Min. age (cal BCE/CE)	Max. age (cal. BCE/CE)	Mean age (cal. BCE/CE)
LuS-16754	20	520 ±30	263	531	1687	1419	1582
Ua-61355	45	866 ±28	573	770	1377	1180	1246
β-508936	91.5	1040 ±30	980	1161	970	789	896
β-508937	102.5	1230 ±30	1101	1240	849	710	785
β-508938	109.5	1260 ±30	1192	1293	758	657	703
Ua-61356	123.5	1612 ±28	1428	1676	522	274	427
LuS-16755	150	2595 ±35	2392	2760	-422	-810	-655
LuS-16756	203	3820 ±35	3997	4333	-2047	-2383	-2219
LuS-16757	275.5	5155 ±40	5677	5985	-3727	-4035	-3891

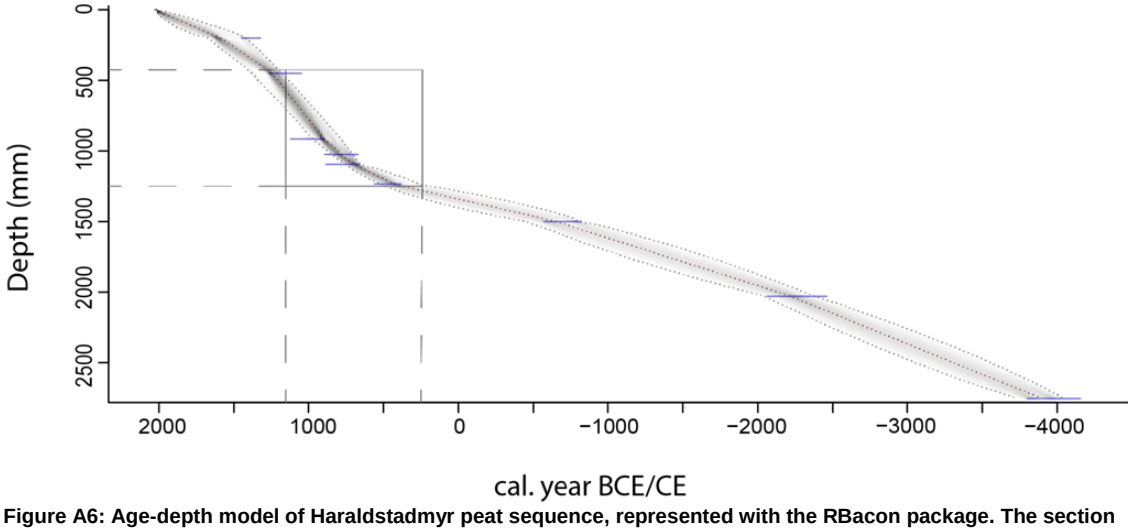

Figure A6: Age-depth model of Haraldstadmyr peat sequence, represented with the RBacon package. The section in the rectangle indicates the study period 250-1150 CE.

The uncalibrated and calibrated radiocarbon ages of Ulbergmyr peat sequence are presented in Table A2. Sample LuS-15686 was discarded, as this sample was found to be older than the sample taken at 108 cm. The year of the coring was excluded during the construction of the age-depth model. As a result, the age-depth model (Fig. A7) was generated based on 5 radiocarbon ages in total.

Table A2: Radiocarbon ages for Ulbergmyr peat sequence.

https://doi.org/10.5194/cp-2022-23
Preprint. Discussion started: 22 March 2022

Lab number	Core depth (cm)	^{14}C age BP	Min. age (cal BP)	Max. age (cal BP)	Min. age (cal BCE/CE)	Max. age (cal. BCE/CE)	Mean age (cal. BCE/CE)
Ua-67047	35	1191 ±29	1229	1024	721	926	822
LuS-15685	52	1455 ±35	1363	1188	587	762	637
LuS-15686	92	1720 ±35					
LuS-15687	108	1715 ±35	1734	1588	216	362	278
LuS-14936	125	1880 ±35	1904	1736	46	214	139
LuS-14935	495	4620 ±40	5542	5115	-3592	-3165	-3423

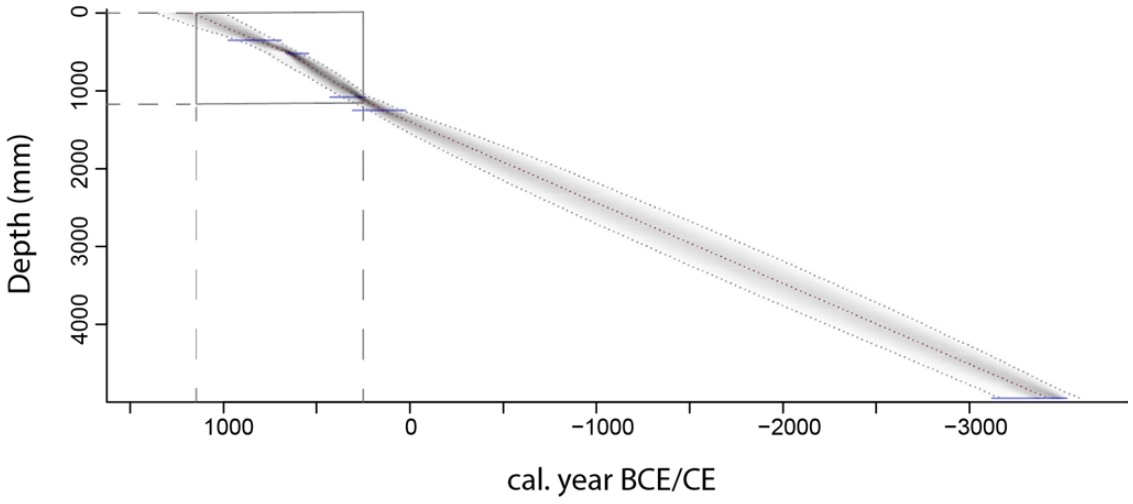

Figure A7: Age-depth model Ulbergmyr peat sequence, represented with the RBacon package. The section in the rectangle indicates the study period 250-1150 CE.

The chronology of Ulbergmyr peat sequence approximately covers the last 3500 years. However, as the bottom of the bog was not reached during the coring, the complete chronology of the bog most likely dates back even further. From 35-52 cm, the mean accumulation measures 0.92 mm/yr. The mean accumulation rate is relatively higher from 52-108 cm in comparison to the rest of the core, namely 1.56 mm/yr. The age-depth model is linear from 108-495 cm, with a mean accumulation rate of 1.05 mm/yr.

The radiocarbon ages of Åsheimmyr peat sequence are listed in Table A3. Sample Ua-72109 was discarded, as this radiocarbon age was found to be too old (Selsing, Lillehammer and Griffin, 1999). The year of the coring was excluded during the construction of the age-depth model.

Table A3: Radiocarbon ages for Åsheim peat sequence

Lab number	Core depth	^{14}C age BP	Min. age	Max. age	Min. age	Max. age	Mean age

https://doi.org/10.5194/cp-2022-23
Preprint. Discussion started: 22 March 2022

	(cm)		(cal BP)	(cal BP)	(cal BCE/CE)	(cal. BCE/CE)	(cal. BCE/CE)
	240	312 ±30	419	807	1531	1143	1409
Ua-72108	320	1147 ±28	966	1172	984	778	898
Ua-72109	360	1664 ±29					
	440	1872 ±31	1730	1988	220	-38	118
Ua-72110	630	3655 ±30	3842	4089	-1892	-2139	-2018

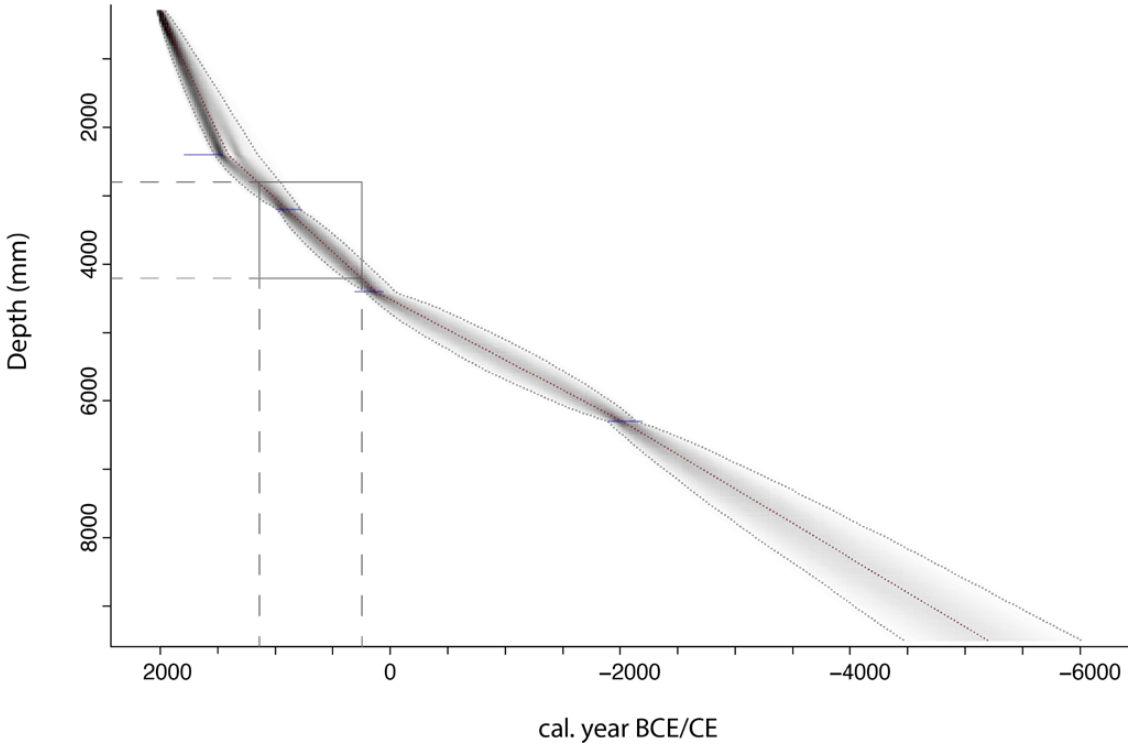

Figure A8: Age-depth model Åsheimmyr peat sequence represented with the RBacon package. The section in the rectangle indicates the study period 250-1150 CE.

Åsheimmyr peat sequence covers over 5000 years (Fig. A8). The mean accumulation rate is the highest at the top of the bog, from 30-240 cm, i.e. 3.54 mm/yr, after which the accumulation rate decreases to 1.55 mm/yr from 240-440 cm. The lower part of the peat sequence, from 440-630 cm has a mean accumulation rate of 0.89 mm/yr.

https://doi.org/10.5194/cp-2022-23
Preprint. Discussion started: 22 March 2022

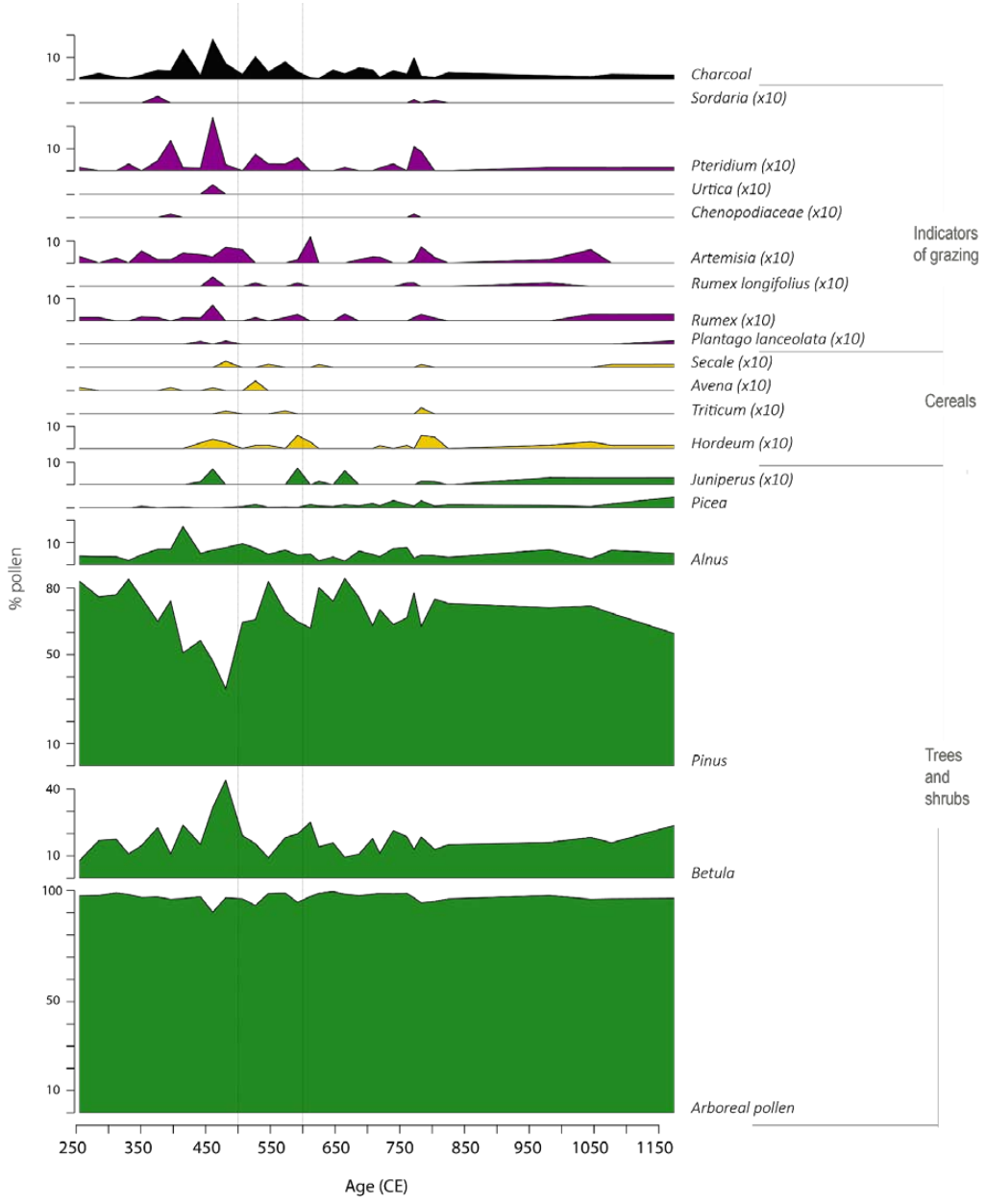

Figure A9. Percentage pollen diagram of Ulbergmyr peat sequence (Fron area), showing a selection of trees, cereals, and other anthropogenic indicators according to cal. age (CE), from 250 BCE to 1150 CE. Pollen types that were multiplied by 10 are indicated with (x10) in the title for each pollen type. Percentages of pollen, spores and non- pollen palynomorphs outside the pollen sum (X) are based on (ΣP+X).

https://doi.org/10.5194/cp-2022-23
Preprint. Discussion started: 22 March 2022

Figure A10. Percentage pollen diagram for Åsheimmyr (Forsand area), showing a selection of trees, cereals, and other anthropogenic indicators according to cal. age (CE), from 250 BCE to 1150 CE. Pollen types that were multiplied by 10 are indicated with (x10) in the title for each pollen type. Percentages of pollen, spores and non-pollen palynomorphs outside the pollen sum (X) are based on (ΣP+X).

https://doi.org/10.5194/cp-2022-23
Preprint. Discussion started: 22 March 2022

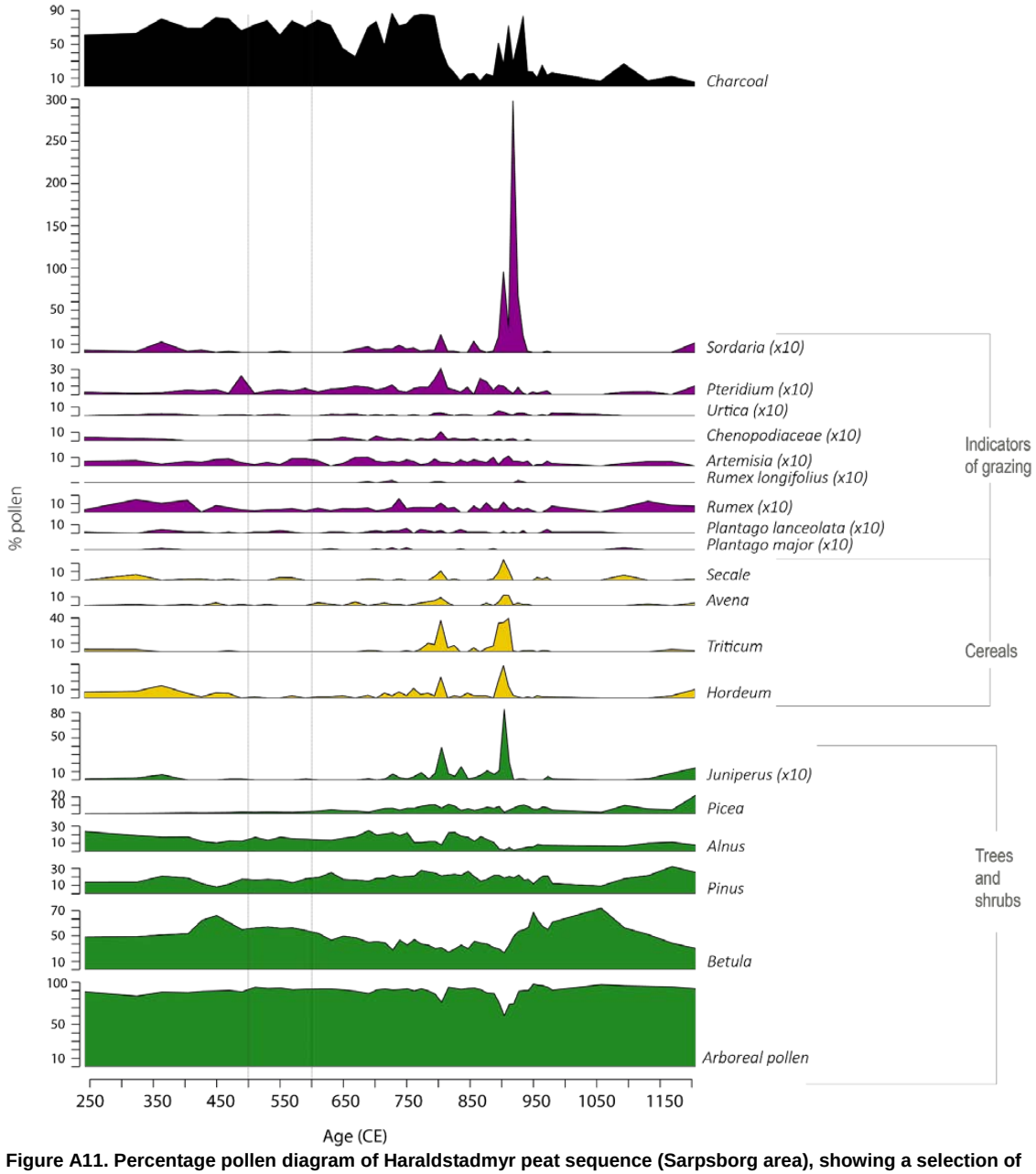

Figure A11. Percentage pollen diagram of Haraldstadmyr peat sequence (Sarpsborg area), showing a selection of trees, cereals, and other anthropogenic indicators according to cal. age (CE), from 250 BCE to 1150 CE. Pollen types that were multiplied by 10 are indicated with (x10) in the title for each pollen type. Percentages of pollen, spores and non- pollen palynomorphs outside the pollen sum (X) are based on (ΣP+X).

https://doi.org/10.5194/cp-2022-23
Preprint. Discussion started: 22 March 2022

Climate of the Past Discussions
Open Access
EGU

Table A4. Information about the proxies and locations marked in Fig. 9.

Location	Coordinates	Type of data	Reference
Tornetrask	68.25° N, 19.6° E	Tree-ring	Grudd, 2008
Northern Scandinavia (NScan)	68° N, 24° E	Tree-ring	Esper et al., 2012
Ulbergmyr, Norway	61.64° N, 9.63° E	Pollen	This study
Åsheimmyr, Norway	58.89° N, 6.22° E	Pollen	This study
Haraldstadmyr, Norway	59.17° N, 11.03° E	Pollen	This study
Forsand, Norway	58.89° N, 6.22° E	Finds of ergot	Løken, 2020
Medelpad, Sweden	62.42° N, 17.05° E	Pollen showing decline agriculture mid-sixth century	Pedersen and Widgren, 2011
Blekinge, Sweden	56.25° N, 15.02° E	Pollen showing decline agriculture mid-sixth century	Pedersen and Widgren, 2011
Gotland, Sweden	57.45° N, 18.97° E	Pollen showing decline agriculture mid-sixth century	Pedersen and Widgren, 2011
Forsand, Norway	58.89° N, 6.22° E	Evidence for site abandonment	Løken, 2020
Fron	61.64° N, 9.63° E	Evidence for site abandonment	Gundersen, 2021
Bjørnstad, Tune	59.17° N, 11.03° E	Evidence for site abandonment	Bårdseth, 2007; Rødsrud, 2007
Öland, Sweden	56.70° N, 16.60° E	Pollen showing decline agriculture mid-sixth century	Pedersen and Widgren, 2011
Gotland, Sweden	57.62° N, 18.55° E	Evidence for site abandonment	Gräslund and Price, 2012
Southern Norway	58.50° N, 8.38° E	Evidence for site abandonment	Solberg, 2000
Southwest Norway	59.43° N, 5.58° E	Evidence for site abandonment	Solberg, 2000
Mälaren valley, Sweden	59.72° N, 16.20° E	Evidence for site abandonment	Löwenborg, 2012